8-2019

Solvent Extraction of Yttrium: Modeling the Rate Coefficient, Loading Ratio and Stoichiometric Ratio

David DeSimone
University of Tennessee

To the Graduate Council:

I am submitting herewith a dissertation written by David DeSimone entitled "Solvent Extraction of Yttrium: Modeling the Rate Coefficient, Loading Ratio and Stoichiometric Ratio." I have examined the final electronic copy of this dissertation for form and content and recommend that it be accepted in partial fulfillment of the requirements for the degree of Doctor of Philosophy, with a major in Chemical Engineering.

Robert Counce, Major Professor

We have read this dissertation and recommend its acceptance:

Jack Watson, Paul Dalhaimer, Sankar Raghavan, Wei Zheng

Accepted for the Council:

Dixie L. Thompson

Vice Provost and Dean of the Graduate School

(Original signatures are on file with official student records.)

Solvent Extraction of Yttrium:
Modeling the Rate Coefficient, Loading Ratio and Stoichiometric Ratio

A Dissertation Presented for the

Doctor of Philosophy

Degree

The University of Tennessee, Knoxville

David DeSimone

August 2019

DEDICATION

To my loving wife, Betsy –

Thank you for your patience, support and reassurances.

To a man's best friend, Charlie –

Thank you for reminding me to take walks and to stop to smell the roses.

To mom and dad –

Thank you for the life lessons that I've used for continual guidance.

ACKNOWLEDGEMENTS

Sincere thanks to Amy Brewer, Rita Gray, Sarah Humphries, Amber Tipton, Lindsi Whitaker and Kerri Cline in the Chemical Engineering Department. Without your support, I would not have entered the graduate program – let alone have completed it. Your daily assistance with logistical concerns and mental motivation has had an incalculable positive effect on my graduate school tenure. Thank you.

Thank you, Dr. Counce, for being an excellent advisor. Your encouragement and mentorship have given me the confidence to conduct research independently and report results effectively. Thank you, Dr. Watson, for your technical expertise. Your contributions ensured that I focused the research on the pertinent conditions and reported the insightful results. Thank you to my other committee members: Paul Dalhaimer, Sankar Raghavan and Wei Zheng. Your feedback and recommendations have been critical both in the classroom and in the lab. Special appreciation is also given to Dr. Bamin Khomami for affording me the opportunity to pursue a graduate degree in Chemical Engineering.

Thank you to Drs. David DePaoli and Barry Spencer of Oak Ridge National Lab, Kevin Lyon of Idaho National Lab and Dr. Patrick Zhang of the Florida Industrial and Phosphate Research Institute. Recognition is also given to Natasha Ghezawi, Thomas Gaetjens, Nicholas Dement, Daniel Taylor Forrest, Samantha Thorpe, Haley Thomasson and Betsy DeSimone of the University of Tennessee for their assistance in the lab.

Financial support for this research was provided by the Graduate Assistance in Areas of National Need Fellowship, the Critical Materials Institute and the Department of Chemical Engineering at the University of Tennessee. I am very thankful to each sponsor for the continuous support.

ABSTRACT

Yttrium was extracted from acidic solutions using di(2-ethylhexyl) phosphate (DEHPA) for three studies. In doing so, three process parameters were analyzed: extraction rate coefficient, loading ratio, and stoichiometric ratio.

The first parameter, extraction rate coefficient, was modeled for a mixer-settler where the organic phase was recycled and the extractant concentration varied. The extraction rate coefficient increased as the recycle ratio increased because recycling the organic phase increased the organic-to-aqueous volume ratio in the mixer and thus increased the interfacial area between phases. The extraction rate coefficient increased as the extractant concentration increased when the extractant concentration was low. However, at high extractant concentrations, the organic phase viscosity had increased due to high metal loading. The high viscosity lowered the organic-phase molecular diffusion and thus decreased the extraction rate coefficient.

Based on process economics, it may be beneficial to conduct a process such that the second parameter, loading ratio, is maximized. This is most likely true for processes using costly extractants. A procedure to determine the maximum loading ratio and corresponding optimum extractant concentration for any solvent extraction process was presented. The previous study's results were used for validation. To increase the loading ratio, operating nearer to the optimum extractant concentration was more effective than increasing the efficiency. An example was presented where although all processes operated at 90% efficiency, the only profitable process was the scenario operating at the optimum extractant concentration.

The third parameter, stoichiometric ratio, was modeled for the equilibrium extraction of yttrium from hydrochloric acid. Although some authors have observed stoichiometric ratios less than the theoretical value of three, few have suggested a mechanism for the deviation

from ideality. This study confirmed that the decrease was attributed to chloride ions complexing with yttrium ions to extract together into the organic phase. The overall equilibrium equation is described as a weighted average of two simultaneous equilibrium extractions. Increasing either the hydrochloric acid concentration or the yttrium feed concentration decreased the stoichiometric ratio, but the former had a more significant effect. The aqueous-phase activity coefficients provided only slight improvements in predicting the equilibrium conditions.

TABLE OF CONTENTS

LIST OF TABLES

LIST OF FIGURES

INTRODUCTION

Three studies were conducted where yttrium was extracted from acidic solutions using di(2-ethylhexyl) phosphate (DEHPA). For each study, an extraction parameter was analyzed and modeled. The first study modeled the extraction rate coefficient, the second study calculated the loading ratio and the third study modeled the equilibrium stoichiometric ratio. These parameters have historically been used as metrics to quantify extraction processes. Therefore, by modeling each parameter, information can be gained as to which factors affect the respective processes and how to alter these factors to achieve the desired extraction results.

The first study modeled the extraction rate coefficient of yttrium from sulfuric acid for a process that recycled the organic phase. After extraction, a portion of the organic phase was returned to the mixer for reprocessing. In doing so, the organic-to-aqueous phase ratio within the mixer was greater than the organic-to-aqueous flow rate ratio. This increased the interfacial area between phases and thus increased the overall extraction rate. This relationship was studied over a series of extractant concentrations to determine how the extraction rate coefficient changed with respect to both recycle ratio and extractant concentration.

The second study provided a means to calculate the loading ratio for any solvent extraction process then used the data from the first study to validate the procedure. The loading ratio is the amount of metal that is extracted per mole of extractant used. It is suggested to define systems in terms of the loading ratio in addition to the efficiency since the efficiency alone has several limitations. It is also shown that there exists an optimum extractant concentration yielding a maximum loading ratio for all extraction processes because the extractant concentration has both a direct and an inverse effect on the loading ratio. The means to calculate this optimum and corresponding maximum are provided. Finally, an example is presented to illustrate the need to consider the maximum loading ratio as a design

consideration. From an economic perspective, maximizing the loading ratio may be beneficial when the extractant cost is significant.

The third study models the stoichiometric ratio for an equilibrium process where yttrium is extracted from hydrochloric acid. Although previous authors have also shown that extraction does not always proceed at the theoretical stoichiometric ratio (3 for yttrium), few have given detailed accounts of the mechanism for this deviation from ideality. The study shows that this deviation is attributed to chloride ions complexing with some of the yttrium ions and extracting into the organic phase with the yttrium as a complex. The overall equilibrium is thus described as a weighted average of both the non-complexing extractions and the complexing extractions that simultaneously occur. A model is developed to predict the overall stoichiometric ratio for the equilibrium extraction given the initial hydrogen and yttrium ion concentrations.

These three independent studies provide guidance for achieving desired extraction results. Each study targeted a specific metric – the extraction rate coefficient, the loading ratio and the stoichiometric ratio. By understanding the scope of each metric and which factors influence each metric, extraction processes can be designed and assessed most effectively.

CHAPTER I

Modeling the Extraction Rate Coefficient for a Process Employing Organic-Phase Recycle

A version of this chapter has been submitted for publication as a journal article:

DeSimone, D., Ghezawi, N., Gaetjens, T., Counce, R., Watson, J. Modeling the Extraction Rate Coefficient for a Process Employing Organic-Phase Recycle. Solvent Extraction and Ion Exchange, 2019.

As lead author of the publication, David DeSimone was responsible for reviewing the literature, designing the experiment, conducting the tests, analyzing the results and writing most of the journal article. Natasha Ghezawi and Thomas Gaetjens assisted with experimental testing. Robert Counce and Jack Watson provided technical expertise, literature recommendations and writing assistance. The version below focuses on developing an empirical model in conjunction with a theoretical model whereas the version submitted for publication focuses solely on the theoretical model.

Abstract

Recycling a portion of the organic phase back to the mixing chamber as it exits the settling chamber allows a mixer-settler to concentrate the extracted product when extractants with very high distribution coefficients are used. Additionally, since most settlers do not operate well at extremely low flow rate ratios, employing this process ensures that a significant amount of the organic phase is present in the settler and thus minimizes entrainment in both outlet phases. In this study, extraction of yttrium (Y) from sulfuric acid was studied using di(2-ethylhexyl) phosphate (DEHPA). A portion of the organic phase was continuously recycled back into the mixer after extraction. By doing so, the mixer operated at a moderate organic-to-aqueous volumetric phase ratio while the overall process used a low organic-to-aqueous flow rate ratio. The objective of the study was to evaluate the effective performance of the mixer when operating at different organic-phase flow fractions. To model the extraction rate coefficient, a 2-factor designed experiment was performed by conducting both batch equilibrium tests and lab-scale mixer-settler tests. The first factor, organic-phase

flow fraction (a function of the fraction recycled), was varied over four discrete levels, while the second factor, extractant concentration, was varied over three discrete levels. Increasing the organic-phase flow fraction yielded a continual increase in the extraction rate coefficient over the experimental domain. In contrast, increasing the extractant concentration yielded an initial increase followed by a subsequent decrease in the extraction rate coefficient. The decline in the extraction rate coefficient at high extractant concentrations was attributed to a decrease in the yttrium-extractant complex's diffusion coefficient. The lower diffusion coefficient was attributed to a high organic-phase dynamic viscosity at high extractant concentrations. The elevated viscosity was attributed to the increased metal loading in the organic phase. Mass transfer resistance was largely (or completely) in the organic phase. The large yttrium-extractant complex was most likely responsible for both the resistance to mass transfer in the organic phase and the high viscosity in the organic phase. Overall, two models are proposed: one with viscosity effects implicitly contained within the extractant concentration and one that explicitly quantifies the viscosity effect. When used in conjunction with the derived equations, the proposed models can be used to estimate the performance of larger mixer-settlers.

Key Words

Mixer-Settler, Recycle, Yttrium, Rate Coefficient, Viscosity

Introduction

Background

Solvent extraction via mixer-settlers has been industrially effective in extracting lanthanides from leach solutions for many years [1]. Recently, many of these lanthanides (referred to as rare earth elements or REE's) have been classified by the U.S. Department of Energy as critical materials for their technological importance, economic value, and potential supply limitations [2]. Because of this, there has been interest in improving solvent extraction

techniques. One proposed method of improvement, recycling at least one of the exiting streams, has been shown to increase efficiency [3-5], reduce emulsions [6], and reduce entrainment [5, 6] when employed correctly. It has been realized that, among other conditions, recycle is advantageous when there is insufficient turbulence in the mixer [7] and when the recycled phase is the phase favored by the REE at equilibrium [3]. This latter case indicates that recycle works best in systems with high distribution coefficients. As previous authors have suggested, when recycle is employed properly, the exiting extract is more concentrated compared to nonrecycled processes. This yields an equivalent efficiency at a lower solvent flow rate [4] and potentially provides for the operability of very low organic-to-aqueous flow ratios. The increased extraction rate observed when recycle is employed has been attributed to the increased dispersed-phase holdup and the increased interfacial area [4, 8, 9] that results. Although recycle models relating the mixer-settler extraction performance to the holdup have been proposed [10], they do not account for changes in the extractant concentration in tandem with changes in the fraction recycled. The purpose of this study was to determine the efficiency and model the extraction rate coefficient for solvent extraction processes that employ recycle over a range of extractant concentrations.

Description of Organic-Phase Recycle

All symbols and nomenclature for the following definitions and derivations are listed in Table 1 in Appendix A. Figure 1 in Appendix B depicts the cross section of a typical mixer-settler. Both the aqueous-phase feed stream and the organic-phase feed stream enter via the mixing chamber then exit from the settling chamber after undergoing phase separation. Figure 2 in Appendix B depicts the process flow diagram for a mixer-settler where a portion of the exiting organic-phase stream is recycled. A fraction of the organic-phase stream was sent back to the mixer while the remainder of the organic-phase stream exited the system. The fraction recycled was defined as the ratio of the recycle stream flow rate to the total organic-phase flow rate entering the mixer:

$$q \equiv \frac{\dot{P}}{\dot{O} + \dot{P}} \qquad (1)$$

where q was the fraction recycled, $\dot{P}$ was the volumetric flow rate of the recycle stream and $\dot{O}$ was the volumetric flow rate of the organic-phase feed stream. The organic-phase flow fraction was defined as the ratio of the organic-phase volumetric flow rate into the mixer to the total volumetric flow rate into the mixer:

$$W \equiv \frac{\dot{O} + \dot{P}}{\dot{O} + \dot{A} + \dot{P}} \qquad (2)$$

where W was the organic-phase flow fraction and $\dot{A}$ was the volumetric flow rate of the aqueous-phase feed stream. The dependence of the organic-phase flow fraction on the fraction recycled was derived by rearranging and substituting equation (1) into equation (2):

$$W = \frac{\dot{O}}{\dot{O} + \dot{A}(1 - q)} \qquad (3)$$

As equation (3) predicts, increasing the fraction recycled resulted in a nonlinear increase in the organic-phase flow fraction. Because extraction efficiency has been shown to increase when the extraction favors the dispersed phase and when the dispersed phase is recycled [3], only the organic phase was recycled for this study. The maximum organic-phase fraction recycled was fixed at 80%. This maximum correlated to an organic-phase flow fraction of 0.33 and was chosen to ensure that the dispersion in the mixer remained aqueous-phase continuous. Previous authors have shown that the onset of the region of ambivalence – where the dispersion may be aqueous-phase or organic-phase continuous – occurs when the holdup of an individual phase exceeds approximately 0.33 [9-11].

Approach

To model the extraction rate coefficient as a function of both the organic-phase flow fraction and the extractant concentration, a two-factor designed experiment was conducted. For the extraction process, DEHPA was the ionic extractant and yttrium (III) sulfate octahydrate was the REE compound. Organic-phase flow fraction consisted of four discrete levels

(corresponding to four fractions recycled) and extractant concentration consisted of three discrete levels (for a total of twelve trials). Extractant concentration refers to the concentration of DEHPA within the organic phase before extraction (in the organic-phase feed stream). Concentrations of DEHPA in other organic-phase streams are notated accordingly. Each trial consisted of a continuous test on the mixer-settler and an equilibrium batch test. All continuous tests and equilibrium tests were conducted at an organic-to aqueous phase ratio of 0.1. To conduct the trials, yttrium (III) sulfate octahydrate (99.9% REO) was obtained from Fisher Scientific and dissociated in 0.2 *M* sulfuric acid to obtain an aqueous-phase feed stream concentration of 1.0 mg yttrium ion per mL of aqueous solution. The aqueous-phase feed stream concentration was held fixed for all trials. The DEHPA (95% purity obtained from Fisher Scientific) and the diluent (Isopar-L obtained from CORECHEM) were mixed to obtain extractant concentrations in the organic-phase feed stream of 0.1 *M*, 0.2 *M*, and 0.4 *M*. The trials were conducted randomly within groups of the extractant concentration. The 0.2 *M* trials were conducted, followed by the 0.4 *M* trials and then the 0.1 *M* trials. The trial run order is depicted in Table 2 in Appendix A. The extractant concentration in the organic feed stream was designated as E. All trials were conducted at 21°C.

Mixer-Settler Test

For the continuous test of each trial, a single stage of a 4-stage Rousselet Robatel UX 1.1 mixer-settler was used. Figures 3A and 3B in Appendix B show the mixer-settler and the overall experimental set-up. The mixing chamber volume was 35 mL while the settling chamber volume was 143 mL. The mixer speed was fixed at 1000 rpm for each trial. The aqueous-phase feed stream entered the mixing chamber at a fixed flow rate of 45.5 mL/min and exited the settling chamber via gravity flow. Similarly, the organic-phase feed stream entered the mixing chamber at a fixed flow rate of 4.5 mL/min and exited the settling chamber via gravity flow. No entrainment was observed in either phase for all trials. After exiting the settling chamber, the fraction recycled was pumped back into the mixing chamber while the nonrecycled fraction exited the system. All flow rates were controlled via Fluid

Metering Inc RH1CKC pump heads with Cole Parmer Masterflex modular drives. For each trial, samples of each process stream were taken at regular time intervals. Each time interval equaled approximately 3 organic-phase turnovers. To determine the concentrations of the aqueous-phase streams, 10 mL of each aqueous-phase sample were diluted with 90 mL of 0.20 *M* sulfuric acid and the resulting specimens were analyzed via inductively coupled plasma optical emission spectrometry (ICP-OES). To determine the concentrations of the organic-phase streams, 10 mL of each organic-phase sample were stripped via a batch process using 5.0 *M* sulfuric acid and an organic-phase to aqueous-phase volume ratio of 0.2. After contact, 40 mL of the acid were diluted with 960 mL of deionized water. The resulting aqueous specimens were analyzed via ICP-OES.

Plots of the exit streams' concentrations versus time for two representative trials are depicted in Figures 4A and 4B in Appendix B. For trial 4 (Figure 4A) the organic stream had a larger yttrium concentration at steady state whereas for trial 12 (Figure 4B) the aqueous stream had a larger yttrium concentration at steady state. To ensure steady state was reached, each test was conducted until concentrations in the exiting streams achieved constant values. For this study, the concentration was considered constant when the percent change in the cumulative moving average of each exit stream was less than 3%. When this target was achieved, the final concentration was used for analysis.

Equilibrium Batch Test

An equilibrium batch test corresponding to each trial was conducted to determine the distribution coefficient and the equilibrium concentrations associated with each trial. The equilibrium test consisted of contacting the aqueous-phase feed stream and the organic-phase feed stream in a closed vessel using the same volumetric phase ratio that was employed for the continuous test (0.1). The vessel was gently rotated about its axis for five minutes to ensure adequate mixing [12]. The dispersion was separated via a separatory funnel. Aqueous-phase and organic-phase samples were prepared and analyzed using the same procedure that was used for preparing and analyzing the continuous test samples.

Results

Murphree Efficiency

The distribution coefficient for each equilibrium test was calculated according to the following equation:

$$D = \frac{C_{org\ eq}}{C_{aq\ eq}} \qquad (4)$$

where D was the distribution coefficient, $C_{org\ eq}$ was the REE mass concentration in the organic phase at equilibrium, and $C_{aq\ eq}$ was the REE mass concentration in the aqueous phase at equilibrium. The calculated distribution coefficients within each extractant concentration were averaged to determine a typical distribution coefficient for that extractant concentration. The distribution coefficients for each trial are listed in Table 3 in Appendix A. Because the organic phase contained no yttrium initially, the mass balance equation around the equilibrium batch test was:

$$C_{aq\ in}V_A = C_{aq\ eq}V_A + C_{org\ eq}V_O \qquad (5)$$

where $C_{aq\ in}$ was the REE mass concentration in the aqueous-phase feed stream, and V_A, V_O were the aqueous-phase and organic-phase volumes, respectively. By rearranging and substituting equation (4) into equation (5), the organic-phase equilibrium concentration was calculated as:

$$C_{org\ eq} = \frac{C_{aq\ in}}{\frac{1}{D} + \frac{V_O}{V_A}} \qquad (6)$$

Similar to equation (5), since the organic-phase feed stream into the mixer-settler did not contain yttrium, the mass balance equation for the steady-state continuous process yielded:

$$C_{org\ out} = \frac{C_{aq\ in} - C_{aq\ out}}{\frac{\dot{O}}{\dot{A}}} \qquad (7)$$

where $C_{org\ out}$ and $C_{aq\ out}$ were the REE mass concentrations in the exiting organic phase and aqueous phase, respectively. The organic-phase Murphree stage efficiency was the ratio of the change in organic-phase concentration in the mixer-settler test to the change in organic-

phase concentration during the equilibrium batch test. For a process without REE's in the organic-phase feed stream, the organic-phase Murphree efficiency simplified to:

$$\varepsilon = \frac{\Delta c_{mixer-settler}}{\Delta c_{equilibrium}} = \frac{C_{org\ out} - C_{org\ in}}{C_{org\ eq} - C_{org\ in}} = \frac{C_{org\ out}}{C_{org\ eq}} \qquad (8)$$

where ε was the organic-phase Murphree stage efficiency and $C_{org\ in}$ was the REE mass concentration in the organic-phase feed stream (equaling zero). Since the volume ratio for the batch tests equaled the volumetric flow rate ratio for the mixer-settler tests $\left(\frac{V_O}{V_A} = \frac{\dot{O}}{\dot{A}}\right)$, equations (6) and (7) were substituted into equation (8) to obtain:

$$C_{aq\ out} = C_{aq\ in} * \left(1 - \frac{\varepsilon * \frac{\dot{O}}{\dot{A}}}{\frac{1}{D} + \frac{\dot{O}}{\dot{A}}}\right) \qquad (9)$$

and

$$C_{org\ out} = C_{aq\ in} * \left(\frac{\varepsilon}{\frac{1}{D} + \frac{\dot{O}}{\dot{A}}}\right) \qquad (10)$$

Equations (9) and (10) depict the concentrations of the streams exiting the mixer-settler as functions of the entering aqueous-phase concentration, the distribution coefficient, the volumetric phase ratio and the Murphree efficiency. These equations are applicable to all extraction systems where the entering organic phase contains no REE's. The Murphree efficiency for each trial was calculated using equations (6) and (8). Trial #9 was omitted from further analysis because the calculated Murphree efficiency exceeded 100%. Excluding this outlier, the Murphree efficiencies ranged from 38% to 91%. Table 3 lists the calculated Murphree efficiency for each trial.

Organic-Phase Extraction Rate Coefficient

One can analyze mixer performance in terms of either the extraction rate coefficient or the stage efficiency. For this study, the extractant rate coefficient was used, but the two parameters are coupled as will be shown in the following discussion. The following organic-phase mass transfer equation introduced the organic-phase extraction rate coefficient [13]:

$$R = (ka) * \Delta c \qquad (11)$$

where R was the mass rate of REE entering the organic phase, ka was the organic-phase extraction rate coefficient, and Δc was the difference between the organic-phase interfacial metal concentration and the organic-phase bulk metal concentration. Evidence that the rate was controlled by resistance in the organic phase will be described later in the discussion of results. The extraction rate coefficient was the product of the organic-phase mass transfer coefficient multiplied by the total interfacial contact area. Equation (11) employs the total interfacial contact area, not the area per mixer volume, to define the extraction rate coefficient. With the REE concentration in the entering organic phase equal to zero, the reaction balance around the organic phase in the mixer was:

$$R = \dot{O} * C_{org\ out} \qquad (12)$$

Substituting equation (12) into equation (11), the extraction rate coefficient was:

$$ka = \frac{\dot{O} * C_{org\ out}}{\Delta c} \qquad (13)$$

The organic-phase concentration difference was defined as:

$$\Delta c \equiv C_{org\ interface} - C_{org\ bulk} \qquad (14)$$

where $C_{org\ interface}$ and $C_{org\ bulk}$ were the organic-phase REE concentrations at the aqueous-organic interface and within the organic-phase bulk fluid, respectively. Assuming equilibrium at the interface, a negligible concentration gradient through the aqueous-phase film, and a well-mixed organic phase, equation (14) was rewritten as:

$$\Delta c = DC_{aq\ out} - C_{org\ out} \qquad (15)$$

By substituting equation (15) into equation (13), the extraction rate coefficient was:

$$ka = \frac{\dot{O} * C_{org\ out}}{DC_{aq\ out} - C_{org\ out}} \qquad (16)$$

By substituting equations (9) and (10) into equation (16), the extraction rate coefficient was:

$$ka = \frac{\dot{O}}{1 + D\left(\frac{\dot{O}}{\dot{A}}\right)} * \frac{\varepsilon}{1 - \varepsilon} \qquad (17)$$

Equation (17) shows how the extraction rate coefficient and the Murphree efficiency are coupled. It is applicable to extraction systems where the resistance to mass transfer lies within the organic phase and the entering organic phase does not contain REE's. Similar relationships between the Murphree efficiency and the extraction rate coefficient have been developed by other authors [14]. Using the Murphree efficiency calculated for each trial and the average distribution coefficient for each extractant concentration, each trial's extraction rate coefficient was calculated via equation (17). Based on its Murphree efficiency, trial #9 was again excluded. Excluding this outlier, the extraction rate coefficients ranged from 1.9 mL/min to 35.0 mL/min. The distribution coefficient, Murphree efficiency and extraction rate coefficient values for each trial are listed in Table 3.

Discussion

Equilibrium

The chemical equilibrium equation describing the batch contact has been postulated as [1, 15]:

$$Y^{3+} + 3\overline{H_2X_2} \leftrightarrow \overline{Y(HX_2)_3} + 3H^+ \qquad (18)$$

where H_2X_2 refers to the dimeric form of DEHPA and the overbars indicate the species resides in the organic phase. This yields the following equilibrium constant equation:

$$K = \frac{\left[\overline{Y(HX_2)_3}\right]}{[Y^{3+}]} * \frac{[H^+]^3}{[\overline{H_2X_2}]^3}$$

where K is the equilibrium constant and the brackets depict molar concentrations. Since the first term on the right side of the equation is represented by the distribution coefficient, the equilibrium constant equation can be rewritten as:

$$K = D * \left(\frac{[H^+]}{[\overline{H_2X_2}]}\right)^3 \qquad (19)$$

Taking the natural logarithm of equation (19) gives:

$$\ln D = 3 \ln\left(\frac{[\overline{H_2X_2}]}{[H^+]}\right) + \ln K \qquad (20)$$

Equation (20) shows that the reaction stoichiometry predicts the distribution coefficient to be proportional to the third power of the equilibrium extractant concentration. As Figure 5 in Appendix B depicts, this relationship was upheld within a 95% confidence interval when compared to the experimental equilibrium data. The line shown on Figure 5 has a slope of approximately 3. The 95% confidence interval for the slope of the equilibrium line was (1.7, 3.1). The distribution coefficient continued to increase by the theoretical stoichiometric factor as the extractant concentration increased.

Organic-Phase Extraction Rate Coefficient

To scale the extraction rate coefficient to an industrial process, it was assumed that a mixer-settler imparting the same turbine diameter/mixer width and specific power input would be used [16]. It is also assumed that scaled processes would not exhibit entrainment of one phase in another phase as the streams exit the settler. Because the reaction rate coefficient used herein employs the total interfacial contact area rather than the area per mixer volume, the extraction rate coefficient would scale according to the following relationship:

$$\left(\frac{ka}{V}\right)_{laboratory} = \left(\frac{ka}{V}\right)_{industrial} \qquad (21)$$

where V is the mixer volume. As indicated previously, the laboratory mixer volume was 35 mL for this study.

It was assumed that all extraction took place within the mixing chamber and at the liquid-liquid interface [9]. For systems such as the one employed herein, where the resistance to mass transfer resides within the organic phase (verified below), equation (17) depicts the extraction rate coefficient of a mixer-settler as a function of the Murphree efficiency, the distribution coefficient, the volumetric phase ratio and the organic-phase flow rate. By substituting the volumetric flow ratio and organic-phase flow rate used in this study into equation (17), the experimental conditions were depicted graphically. Figure 6 in Appendix B shows the relationship between the extraction rate coefficients, the Murphree efficiencies and the extractant concentrations employed in this study. As the Murphree efficiency

increased, the extraction rate coefficient increased at an increasing rate. However, as equation (17) indicates, the extraction rate coefficient decreased as the extractant concentration increased. Therefore, when no other factors were present, the greatest extractant rate coefficient values occurred during the trials exhibiting high Murphree efficiencies and low extractant concentrations. After the Murphree efficiency was calculated via equation (8), the corresponding extraction rate coefficient was determined from equation (17).

The standard least squares method was used to develop a model relating the extraction rate coefficient to the two experimental factors: organic-phase flow fraction and extractant concentration. The 11 data points were used together to develop a single model that spanned the full range of organic-phase flow fractions and extractant concentrations. Several model iterations were sequentially tested using JMP software. Figures 11, 12 and 13 in Appendix C depict the iterations trialed to achieve the desired model. During the first iteration (Figure 11), a full second-degree polynomial model for the extraction rate coefficient was proposed. Based on the recommended Box-Cox power transformation of this model, the natural logarithm of the extraction rate coefficient was modeled next (Figure 12). Beginning again with a full second-degree polynomial and using backward elimination with a p-value cutoff of 0.05, the following extraction rate coefficient model was ultimately selected (Figure 13):

$$ka = 0.1726 * exp^{-57.15E^2+28.06E+4.52} \qquad (22)$$

As shown in equation (22), the best fit for the extraction rate coefficient was depicted as an exponential model containing both a first-order term for the organic-phase flow fraction and a quadratic term for the extractant concentration. The model had a coefficient of correlation equal to 0.81 and a root mean square error (RMSE) equal to 0.59. The model p-value was 0.01. Each term in the model was deemed significant using a p-value of 0.05. The model suggested that both the organic-phase flow fraction and the extractant concentration affect the extraction rate coefficient for yttrium extraction.

Using the model, the range of the laboratory-scale extraction rate coefficients was estimated for the experimental domain. Figure 7 in Appendix B depicts the extraction rate coefficient as a function of the organic-phase flow fraction for each of the extractant concentrations. The 11 trials are represented by each of the observed data points while the model presented in equation (22) is graphically depicted as the family of predicted curves. Each curve in Figure 7 is not a separate model. The three curves together represent the equation (22) model.

The greatest extraction rate coefficients were observed at the highest organic-phase flow fractions. Since the interfacial contact area between the two phases increased as the organic-phase flow fraction increased [17-19], high extraction rate coefficients were observed at high fractions recycled. As concluded by other authors, this effect would be particularly beneficial for a process employing a low organic-phase feed stream flow rate or a process requiring a concentrated organic-phase product stream [4]. The continual increase of ka as a function of the organic-phase flow fraction is depicted by the first-order term for W in the model. This study employed a maximum organic-phase flow fraction of 0.33 (corresponding to a fraction recycled of 80%). Larger fraction recycled values yield larger extraction rate coefficients if the organic phase remains dispersed within aqueous phase. If increasing the fraction recycled causes the system to enter the region of ambivalence, additional care should be exercised to ensure the organic phase remains dispersed within the aqueous phase.

The extraction rate coefficients were greatest for the trials conducted with extractant concentrations equal to 0.2 *M*. For relatively low extractant concentrations, increasing the extractant concentration increased the extraction rate coefficient (as seen by comparing the solid line to the dotted line in Figure 7). However, after an optimum was reached, further increasing the extractant concentration resulted in a decrease in the extraction rate coefficient (as seen by comparing the dotted line to the dashed line in Figure 7). The decrease in the extraction rate coefficient that was observed at high extractant concentrations was not caused by the reaction equilibrium. The equilibrium results (depicted in Figure 5) showed that the

highest extractant concentration yielded the most extraction whereas the mixer-settler results showed that the highest extractant concentration yielded the lowest extraction rate coefficient. The equilibrium results indicated that the interfacial concentration of the $\overline{Y(HX_2)_3}$ complex continued to increase for each successive extractant concentration. Therefore, the low Murphree efficiencies (and thus the low extraction rate coefficients) observed for the 0.4 *M* trials conducted on the mixer-settler were not attributed to equilibrium conditions. Since casual observations indicated that the viscosity increased during extraction, viscosity measurements were conducted on batch test samples. The purpose of testing the viscosity was to determine what effects (if any) the dynamic viscosity had on the Murphree efficiency and the extraction rate coefficient.

Viscosity

It was observed that the organic-phase viscosity increased with increased extractant concentration. This was especially apparent when the concentration increased from 0.2 *M* to 0.4 *M*. Because the viscosity and the diffusion coefficient are inversely related [20], this observation suggested that the diffusion coefficient of the extracted yttrium specie in the organic phase had decreased as the extractant concentration had increased. As further described below, this was the strongest evidence that the resistance to mass transfer was limited by the diffusion within the organic phase.

Since the effects of high metal concentrations on solvent viscosity had been explored previously [1, 21], dynamic viscosity tests were conducted on samples of the organic phase for each extractant concentration at equilibrium. To see how the organic-phase dynamic viscosity increased during extraction, an Omega Engineering Rotational Viscometer was used to measure the organic-phase dynamic viscosity before and after each equilibrium batch test. The dynamic viscosity of the diluent alone was also measured. The dynamic viscosity results and the corresponding yttrium concentrations at equilibrium are summarized in Table 4 in Appendix A. The dynamic viscosity is represented by μ and the values are reported in centipoise (cP).

Although the dynamic viscosity increased slightly during the batch test for both the 0.1 *M* and 0.2 *M* trials, it increased substantially during the 0.4 *M* trial. Based on how the viscosities increased after the batch tests, the data indicated two main points. First, the viscosity was highly dependent on the concentration of yttrium in the organic phase. Secondly, there was a nonlinear trend between the extractant concentration and the equilibrium viscosity – for each sequential extractant concentration, the equilibrium dynamic viscosity increased at an increasing rate. The first point indicates that the viscosity of the organic phase increases during extraction. The second point indicates that further extraction might not be affected by the organic-phase viscosity until a specific threshold has been reached. As Table 4 indicates, the equilibrium viscosity did not increase significantly when the extractant concentration doubled from 0.1 *M* to 0.2 *M*. However, it increased by a factor of 5 when the extractant concentration doubled again from 0.2 *M* to 0.4 *M*. Had tests within this interval been conducted, the organic-phase dynamic viscosity would begin to increase rapidly after a certain threshold between 0.2 *M* and 0.4 *M* was reached. As explained below, after this threshold concentration is reached, the reaction rate coefficient decreases.

To explain how the equilibrium viscosity of the 0.4 *M* samples was extremely high compared to that of the 0.1 *M* and 0.2 *M* samples, it is important to first remember that the organic-phase molecules had reacted at the aqueous-organic interface as described by the equilibrium results. However, since the $\overline{Y(HX_2)_3}$ molecules were appreciably larger than the other molecules in the system [22], and they were contained within the viscous organic phase, these molecules were especially slow to diffuse from the interface and into the bulk of the organic phase for additional extraction. The slow diffusion of $\overline{Y(HX_2)_3}$ into the bulk organic phase resulted in a large concentration of this molecule at the interface. This build-up at the interface resulted in a decreased yttrium concentration difference at the interface and thus decreased the extraction rate coefficient. Again, this phenomenon verified the premise that the resistance to mass transfer was limited by the diffusion within the organic phase and thus verified the applicability of equation (17). As described by the Wilke-Chang relationship,

the diffusion coefficient is inversely proportional to both the dynamic viscosity of the host solution and the molar volume of the molecule itself [20]. Therefore, the diffusion coefficient of the $\overline{Y(HX_2)_3}$ molecule was significantly lower for the trials conducted at 0.4 *M* as compared to the trials conducted at 0.1 *M* and 0.2 *M*.

The model in equation (22) implicitly contains the viscosity effect in the form of the quadratic term for extractant concentration. The model suggests that the extraction rate coefficient initially increases as the extractant concentration increases. However, when the threshold extractant concentration is reached, the viscosity of the organic phase increased significantly, and the extraction rate coefficient decreased. The equation (22) model offers the reader a simplified approach to estimating the extraction rate coefficient without knowing the equilibrium dynamic viscosity.

With the data presented in Table 4, a relationship between the organic-phase dynamic viscosity and the yttrium concentration was developed. As previously discussed, the viscosities increased after the batch tests and the data indicate that the viscosity is dependent on the concentration of yttrium in the organic phase. Figure 8 in Appendix B shows that a plot of $\frac{1}{\mu^2}$ at equilibrium versus $C_{org\ eq}$ yields an approximately straight line. By fitting a standard least squares regression model to the data in Table 4, the dynamic viscosity can be predicted over the experimental range via the following relationship:

$$\mu = \sqrt{\frac{1}{0.07 - 10.13 * C_{org\ eq}}} \qquad (23)$$

As equation (23) suggests, over the range of experimental conditions, the square of the viscosity is inversely proportional to the yttrium concentration in the organic phase exiting the mixer-settler. In practicality, this suggests that as the organic phase approaches its yttrium-carrying capacity (or maximum concentration), the viscosity increases very rapidly.

The organic-phase equilibrium viscosity can be determined experimentally or by employing equation (23). In doing so, the dynamic viscosity can be used with the extractant concentration and organic-phase flow fraction to develop an alternative model for the extraction rate coefficient. The reader may use this additional model (as opposed to equation (22)) to estimate the extraction rate coefficient when the extractant concentration, organic-phase flow fraction and the dynamic viscosity at equilibrium are known.

To present this alternative method, the natural logarithm of each trial's extraction rate coefficient was plotted as a function of the organic-phase flow fraction. Individual regression lines were plotted for each extractant concentration. Using partial least squares regression analysis, each line was fixed to pass through the origin and employed only the data points associated with a single extractant concentration. Figure 9 in Appendix B depicts the plot and the three partial least squares regression fits – one fit for each extractant concentration. The slope for the 0.1 *M* model (solid line) is approximately 7 whereas the slope for the 0.2 *M* model (dotted line) is approximately 12. For these points associated with these two extractant concentrations, the extraction rate coefficient approximately doubled as the extractant concentration doubled. This suggested that the extraction was diffusion controlled in the organic phase or followed first-order kinetics. However, as discussed previously, this trend did not continue at higher extractant concentration values. The slope for the 0.4 *M* model (dotted line) is approximately 4.5. As mentioned above, this dramatic decrease in the extraction rate coefficient confirmed that the viscosity effect was present at high extractant concentrations.

By dividing the extraction rate coefficient by the extractant concentration and multiplying by the equilibrium dynamic viscosity, the pertinent variables were lumped into one parameter $\left(\frac{ka*\mu}{E}\right)$ for each trial. Figure 10 in Appendix B depicts the natural log of this lumped parameter as a function of the organic-phase flow fraction. The lumped parameter tightly clustered the data points at each organic-phase flow fraction. This indicated that a large portion of the variability between extractant concentrations was described by the

lumped parameter. The linear trend derived from all 11 data points is depicted on Figure 10. The natural log of the lumped parameter continuously increased as the organic-phase flow fraction increased. This increase suggests that the interfacial area increased as the organic-phase flow fraction increased. This is consistent with previous authors' findings [4, 8, 9]. Note also that there was no disruption or transition from the increasing trend. This provides further evidence that all trials were conducted with the organic phase as the dispersed phase; there was no change in the continuous phase.

The linear trend on Figure 10 provides the alternative correlation to the equation (22) model. Using this trend, the reader can predict the mixer performance, the extraction rate coefficient and the factors affecting the extraction rate. With the effects of the distribution coefficient and the viscosity accounted for within the lumped parameter, the increasing trend represents the effects of the organic phase flow fraction over the given range. The organic-phase flow fractions employed in this study cover the range most likely to be of interest. Most settlers are not effective below organic-to-aqueous phase ratios of 0.1. Over this range, the extraction rate coefficient increases with increasing flow fraction, but the slope is relatively modest.

Although this study fixed the yttrium concentration in the aqueous feed stream for all trials, use of Figure 10 for alternative concentrations would be a reasonable, albeit untested, approach. To use the trend for different yttrium concentrations, the ratio of the concentration of interest to the concentration used for this study (0.001 g/mL) must be raised to the third power, as dictated by equation (20). This value would be multiplied by the value obtained from Figure 10 to scale the extraction rate coefficient accordingly. Likewise, the equilibrium conditions (including the distribution coefficient and dynamic viscosity) for the concentration of interest would need to be determined. For lower yttrium concentrations in the aqueous feed stream, the organic phase viscosity would be lower because the equilibrium concentration of yttrium in the organic phase would be lower. Thus, for extracting yttrium at low aqueous feed stream concentrations, using higher extractant concentrations may be

more desirable. Conversely, a lower extractant concentration is most likely necessary when extracting from an aqueous feed stream with a high yttrium concentration.

Although yttrium was used for this study, many rare earth elements would behave similarly. Other 3+ metal ions would form similar complexes (consisting of the rare earth ion surrounded by three extractant molecules), so they would most likely experience lower diffusion coefficients at high extractant concentrations as well (since the diffusion coefficient is largely dependent on molecular volume). Again, the equilibrium conditions would need to be verified for each REE. Corrections for the aqueous feed stream concentrations could also be made as described above. Finally, although it is not advised to extrapolate far beyond the experimental data, it may be reasonable to use Figure 10 to estimate extraction rate coefficients for REE mixtures. As a qualitative guide, the viscosity would depend on the total metal loading in the organic phase, rather than the concentration of an individual element.

Again, when the dynamic viscosity cannot be determined, the reader is advised to employ the model depicted in equation (22). However, the trend depicted in Figure 10 may yield more widely applicable results if the viscosity can be experimentally or empirically determined. Both the equation (22) model and the Figure 10 trend employ units depicted in Table 1 in Appendix A.

Conclusion

It was observed that recycling the organic phase increased the extraction rate coefficient over the experimental domain. Recycling could be a promising way to utilize extractants with high distribution coefficients to concentrate extracted metal ions. The extraction rate coefficient achieved a maximum value over the range of extractant concentrations used. The low extraction rate coefficients at the high extractant concentration were attributed to high viscosity and low organic-phase diffusion at this condition. For systems where the resistance

to mass transfer resides within the organic phase, it is recommended to operate the process at the greatest extractant concentration that does not yield viscosity effects. To do so, two models have been presented. The first model predicts the extraction rate coefficient for a given extractant concentration and organic phase flow fraction whereas the second model yields the desired output if these two inputs plus the organic phase dynamic viscosity are known.

References

1. Xie, F., et al., A critical review on solvent extraction of rare earths from aqueous solutions. Minerals Engineering, 2014. 56: p. 10-28.
2. Critical Materials Strategy. 2011.
3. Treybal, R.E., Recycle in liquid extraction. I&EC Fundamentals, 1964. 3(3): p. 185-188.
4. Kaul, A. and K. VanWormer, Effects of Internal Stage Recycle on Efficiency and Performance of a Mixer-Settler. Ind. Eng. Chem. Process Des. Dev, 1985. 24(3): p. 636-646.
5. Rowden, G.A., J.B. Scuffham, and G.C.I. Warwick, The Effect of Change in Operating Organic/Aqueous Ratio on the Operation of a Mixer-Settler. Proceedings International Solvent Extraction Conference, 1974. 1: p. 81.
6. Ryon, A.D. and R.S. Lowrie, Experimental basis for the design of mixer settlers for the Amex solvent extraction process. 1963.
7. Davis, A.T. and T.J. Colven, The Effect of Mixer Design on the Efficiency of a Pump-Mix Mixer Settler. AIChE Journal, 1961. 7(1): p. 72-77.
8. Hatton, T.A., et al., An Internal Recycle Mixer for Solvent Extraction. Mass Transfer Characterization with Liquid Surfactant Membranes. Ind. Eng. Chem. Fundamentals, 1983. 22: p. 27-35.
9. Pinto, G.A., et al., Design optimization study of solvent extraction - chemical reaction, mass transfer and mixer-settler hydrodynamics. Hydrometallurgy, 2004. 74: p. 131-147.
10. Hoh, Y., S. Ju, and T. Chiu, Effect of Internal Recycle on Mixer-Settler Performance. Hydrometallurgy, 1989. 23: p. 105-118.
11. Holland, F.A. and F.S. Chapman, Liquid Mixing and Processing in Stirred Tanks. 1966, New York: Reinhold Pub. Corp.
12. Product Properties Test Guidelines - Partition Coefficient Shake Flask Method. 1996.
13. Seader, J.D. and H. E., Separation Process Principles. 2nd ed. 2006.

14. Oh, W.J., D.P. Ju, and C. Kim, Analysis of the steady state behavior of a mixer settler. Korean Journal of Chemical Engineering, 1985. 2(2): p. 103-109.

15. Mason, G.W., I. Bilobran, and D.F. Peppard, Extraction of U(IV), Th(IV), Am(III) and Eu(III) by bis para-octylphenyl phosphoric acid in benzene diluent. Journal of Inorganic Nuclear Chemistry, 1978. 40: p. 1807-1810.

16. DeSantana, A.O. and C.C. Dantas, Scale-up of the mixer of a mixer-settler model used in a uranium solvent extraction process. Journal of Radioanalytical and Nuclear Chemistry, 1995. 189(2): p. 257-268.

17. Takahashi, K. and H. Takeuchi, Holdup of Dispersed Phase in a Mixer-Settler Extraction Column. Journal of Chemical Engineering of Japan, 1990. 23(1): p. 12-17.

18. Quadros, P. and C.M.S.G. Baptista, Effective interfacial area in agitated liquid–liquid continuous reactors. Chemical Engineering Science, 2003. 58: p. 3935-3945.

19. Hosseinzadeh, M., M. Ranjbar, and M. Alizadeh, Effect of operational parameters and internal recycle on rhenium solvent extraction from leach liquors using a mixer-settler. Engineering Science and Technology, an International Journal, 2014. 17(2): p. 45-49.

20. Wilke, C.R. and P. Chang, Correlation of Diffusion Coefficients in Dilute Solutions. AIChE Journal, 1955. 1(2): p. 264-270.

21. Ferraro, J.R. and D.F. Peppard, Structural Aspects of Organophosphorus Extractants and Their Metallic Complexes as Deduced from Spectral and Molecular Weight Studies. Nuclear Science and Engineering, 1963. 16: p. 389-400.

22. Marie, C., B. Hiscox, and K. Nash, Characterization of HDEHP-lanthanide complexes formed in a non-polar organic phase using 31-P NMR and ESI-MS. Dalton Trans, 2012. 41: p. 1054-1064.

Appendix A

Table 1: Chapter I Symbols, Notation and Units

Symbol	Definition	Units
$\dot{A}$	Volumetric Flow Rate of Aqueous-Phase Feed Stream	$\frac{mL_{aq}}{min}$
$C_{aq\ eq}$	REE Concentration in Aqueous Phase at Equilibrium	$\frac{g_{REE}}{mL_{aq}}$
$C_{aq\ in}$	REE Concentration in Aqueous Phase Entering System	$\frac{g_{REE}}{mL_{aq}}$
$C_{aq\ out}$	REE Concentration in Aqueous Phase Exiting System	$\frac{g_{REE}}{mL_{aq}}$
$C_{org\ eq}$	REE Concentration in Organic Phase at Equilibrium	$\frac{g_{REE}}{mL_{org}}$
$C_{org\ in}$	REE Concentration in Organic Phase Entering System	$\frac{g_{REE}}{mL_{org}}$
$C_{org\ out}$	REE Concentration in Organic Phase Exiting System	$\frac{g_{REE}}{mL_{org}}$
Δc	Organic-Phase Concentration Difference	$\frac{g_{REE}}{mL_{org}}$
D	Distribution Coefficient	$\frac{mL_{aq}}{mL_{org}}$
E	Extractant Concentration	$\frac{mol_{extractant}}{L_{org}}$
K	Equilibrium Constant	-
ka	Organic-Phase Extraction Rate Coefficient = Mass Transfer Coefficient * Interfacial Contact Area	$\frac{mL_{org}}{min}$
$\dot{O}$	Volumetric Flow Rate of Organic-Phase Feed Stream	$\frac{mL_{org}}{min}$
$\dot{P}$	Volumetric Flow Rate of Organic-Phase Recycle Stream	$\frac{mL_{org}}{min}$

Table 1 (Continued)

Symbol	Definition	Units
q	Fraction Recycled	-
R	REE Mass Transfer Rate	$\frac{g_{REE}}{min}$
V	Mixer Volume	mL_{total}
V_A	Volume of Aqueous Phase	mL_{aq}
V_O	Volume of Organic Phase	mL_{org}
W	Organic-Phase Flow Fraction	$\frac{mL_{org}}{mL_{total}}$
ε	Organic-Phase Murphree Efficiency	-
μ	Organic-Phase Dynamic Viscosity	cP

Table 2: Designed Experiment Run Order

Trial #	E (*M*)	q	W
1	0.20	80%	1/3
2	0.20	60%	1/5
3	0.20	20%	1/9
4	0.20	0%	1/11
5	0.40	60%	1/5
6	0.40	80%	1/3
7	0.40	0%	1/11
8	0.40	20%	1/9
9	0.10	0%	1/11
10	0.10	20%	1/9
11	0.10	80%	1/3
12	0.10	60%	1/5

Table 3: Trial Results Grouped by Increasing Extractant Concentration

Trial #	E	W	D	$D_{average}$	ε	ka
9	0.10	1/11	1.30	1.23	~~1.12~~	~~38.46~~
10	0.10	1/9	1.59		0.45	3.27
12	0.10	1/5	0.98		0.38	2.49
11	0.10	1/3	1.06		0.75	11.86
4	0.20	1/11	4.12	3.70	0.50	3.36
3	0.20	1/9	3.89		0.75	9.77
2	0.20	1/5	3.53		0.79	12.39
1	0.20	1/3	3.26		0.91	35.03
7	0.40	1/11	15.42	19.73	0.62	2.55
8	0.40	1/9	23.59		0.77	5.07
5	0.40	1/5	18.23		0.55	1.90
6	0.40	1/3	21.67		0.69	3.33

Table 4: Organic-Phase Dynamic Viscosities and Yttrium Concentrations

E (*M*)	μ (cP) Before Extraction	μ (cP) At Equilibrium	$C_{org\ eq}\left(\frac{g_{yttrium}}{mL_{org}}\right)$
0.00	3.7	3.7	0.0000
0.10	3.7	4.4	0.0011
0.20	3.7	4.6	0.0027
0.40	4.0	23.0	0.0066

Appendix B

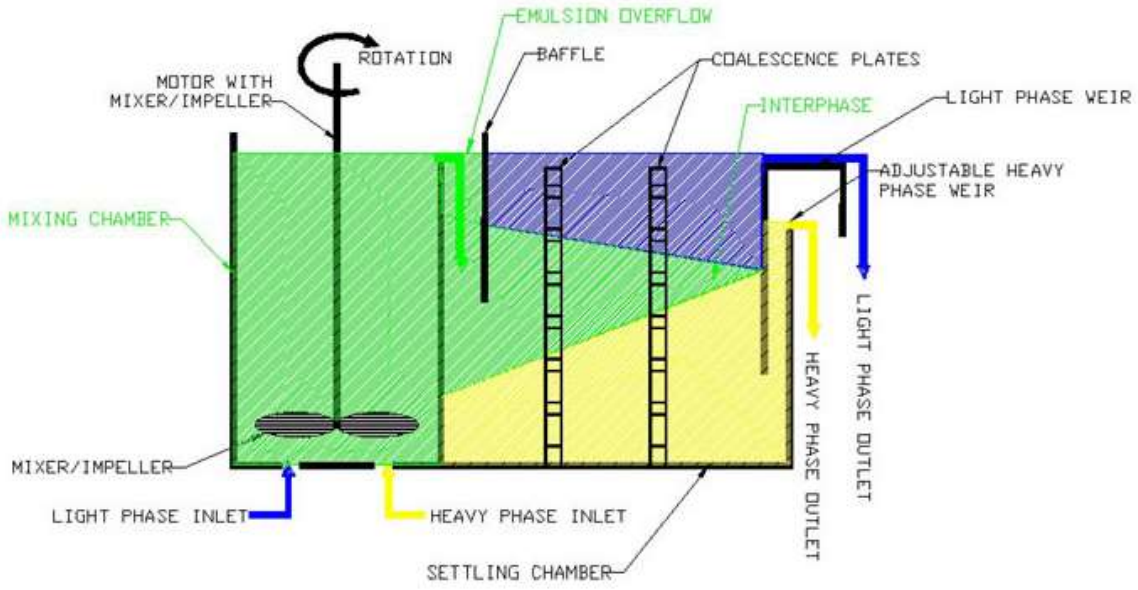

Figure 1: Cross-Section of Mixer-Settler Stage (courtesy of Rousselet-Robatel)

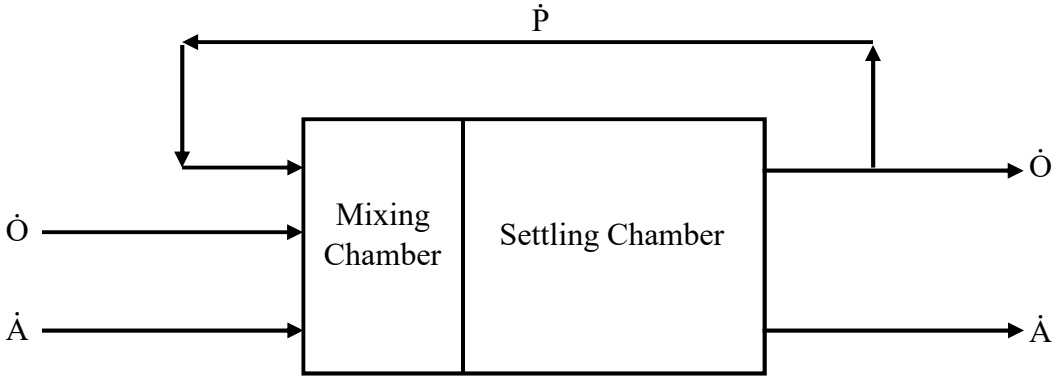

Figure 2: Mixer-Settler Employing Organic-Phase Recycle

Figure 3A: 4-Stage UX 1.1 Mixer-Settler Used (Only 1 Stage Employed for Study)

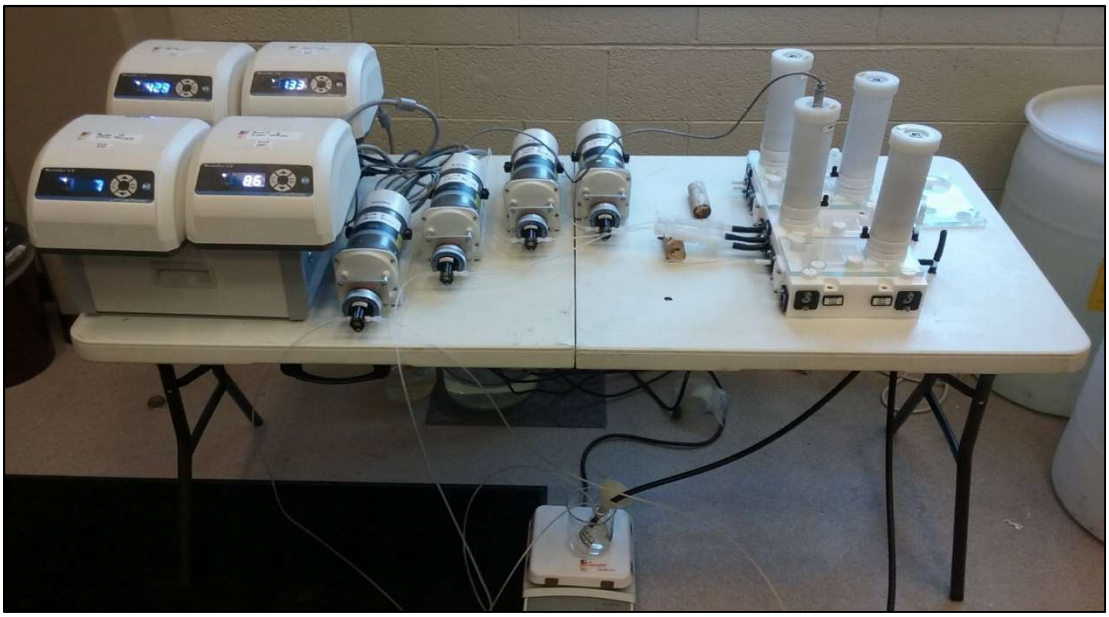

Figure 3B: Mixer-Settler Process Set-Up

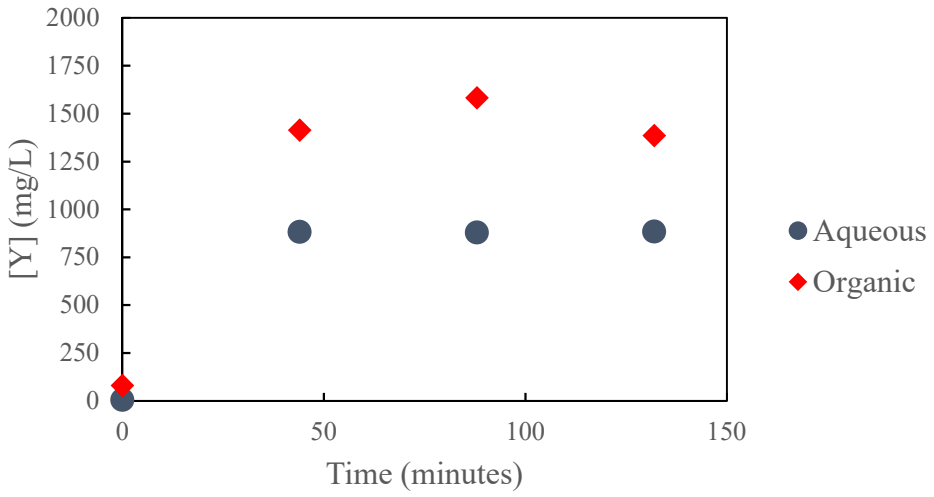

Figure 4A: Trial 4 – Yttrium Concentrations in Mixer-Settler Exit Streams vs Time (E = 0.2 *M*, 0% Recycle)

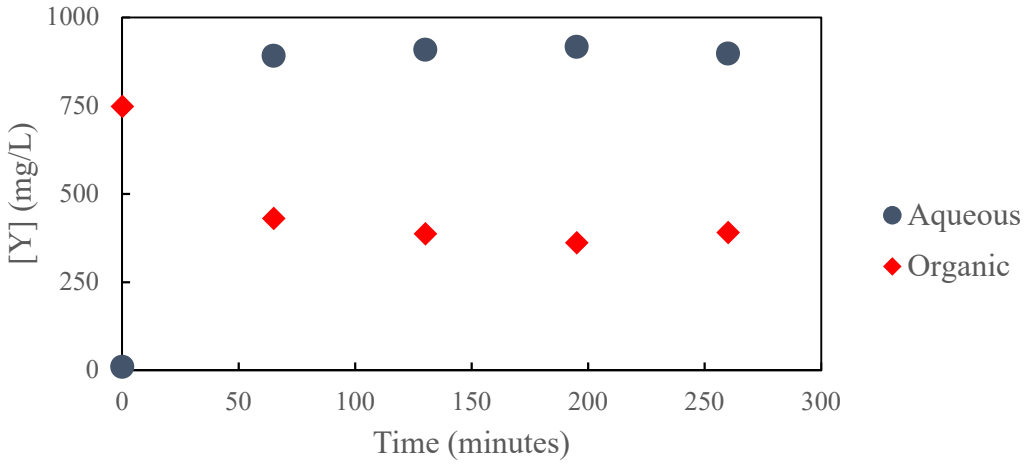

Figure 4B: Trial 12 – Yttrium Concentrations in Mixer-Settler Exit Streams vs Time (E = 0.1 *M*, 60% Recycle)

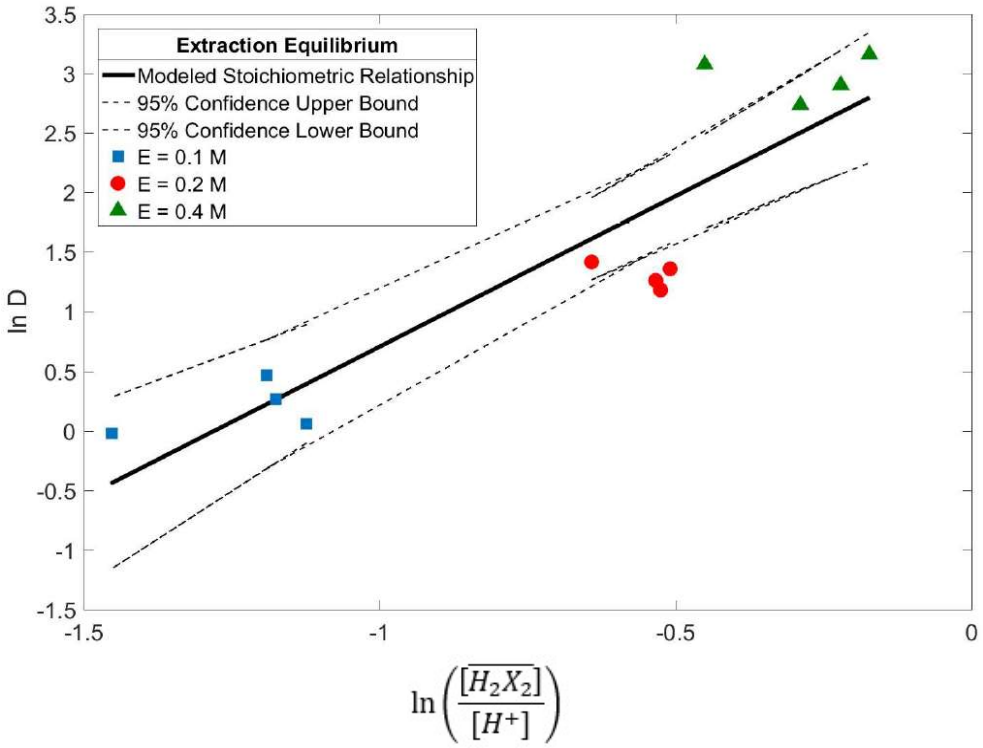

Figure 5: Equilibrium Extraction of Yttrium by DEHPA

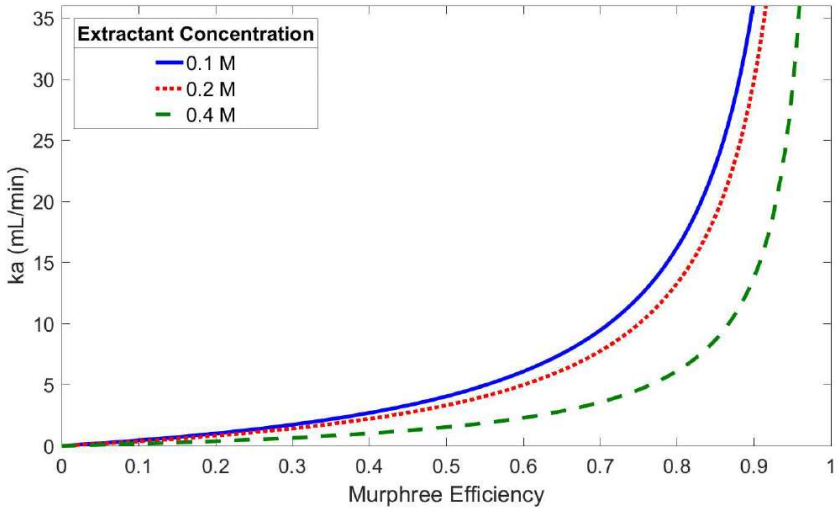

Figure 6: Visualization of Equation (17) for the Experimental Process Parameters

$$\left(\frac{\dot{O}}{\dot{A}} = \mathbf{0.1};\ \dot{O} = \mathbf{4.55}\,\frac{mL}{min}\right)$$

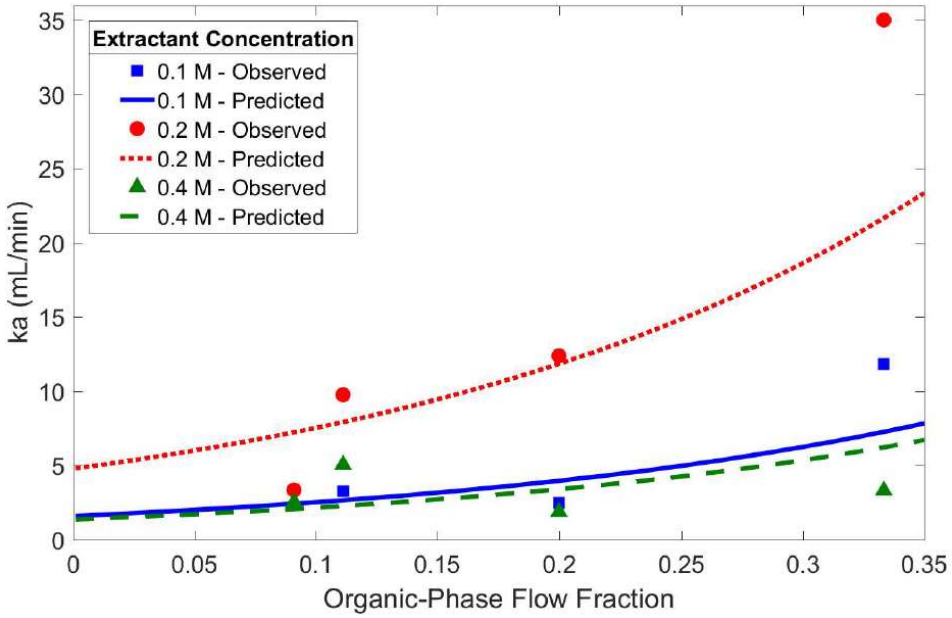

Figure 7: Extraction Rate Coefficient vs Organic-Phase Flow Fraction for Yttrium Extraction by DEHPA

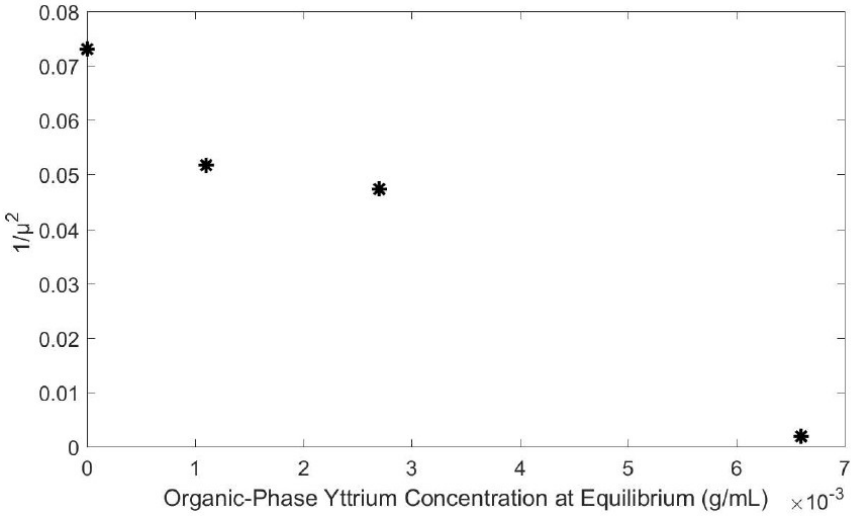

Figure 8: Inverse of Viscosity Squared vs Yttrium Concentration for Organic Phase at Equilibrium

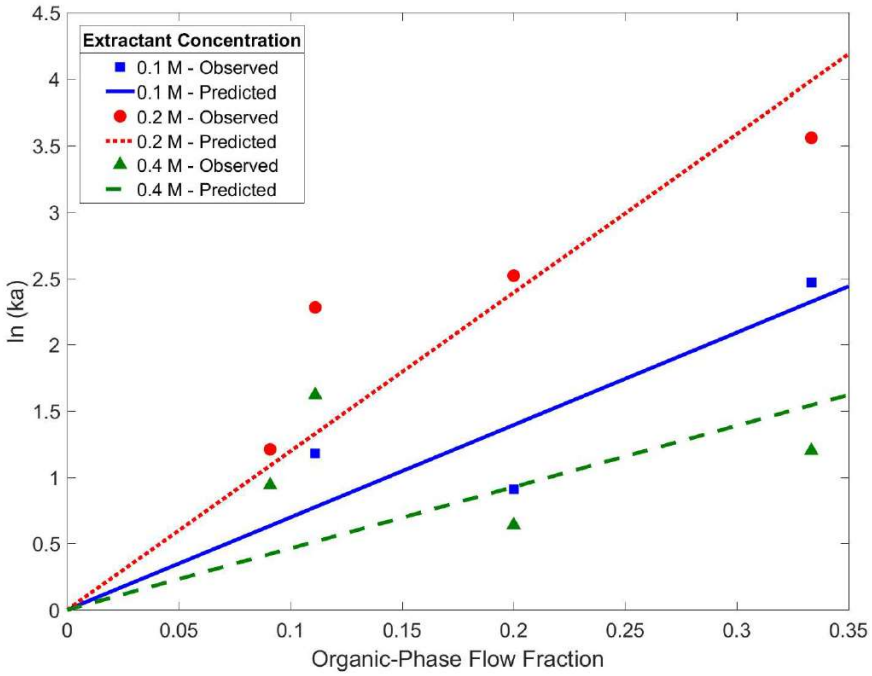

Figure 9: Natural Log of Extraction Rate Coefficient vs Organic-Phase Flow Fraction for Yttrium Extraction by DEHPA

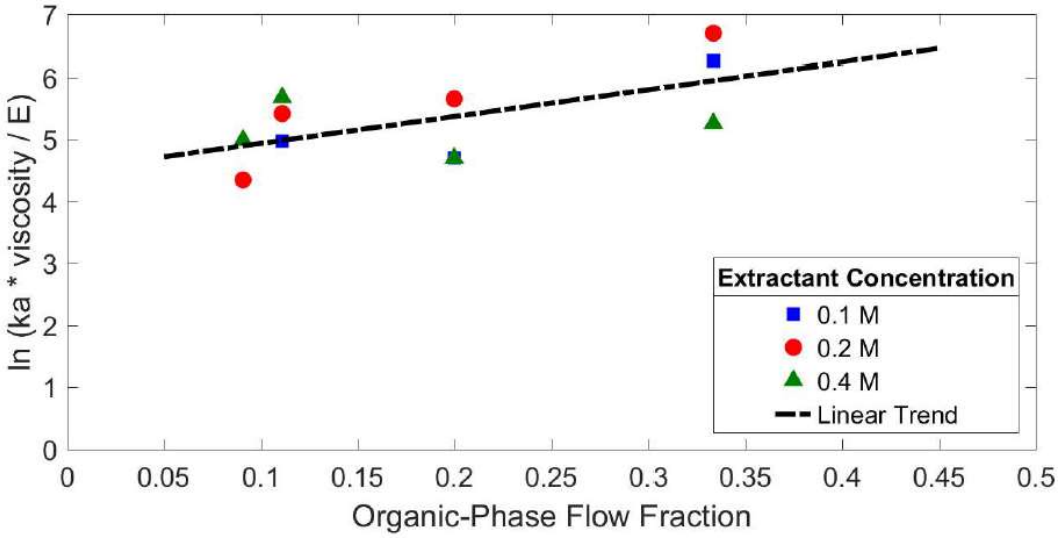

Figure 10: Natural Log of the Lumped Parameter vs Organic-Phase Flow Fraction for Yttrium Extraction by DEHPA

Appendix C

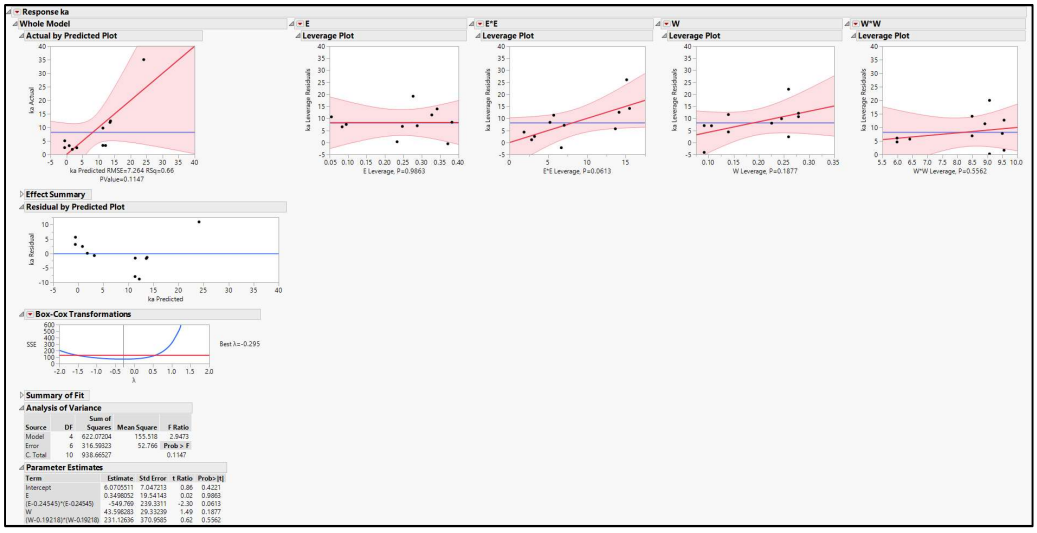

Figure 11: First Iteration of Extraction Rate Coefficient Model

Response: ka; Factors: E^2, E, W^2, W

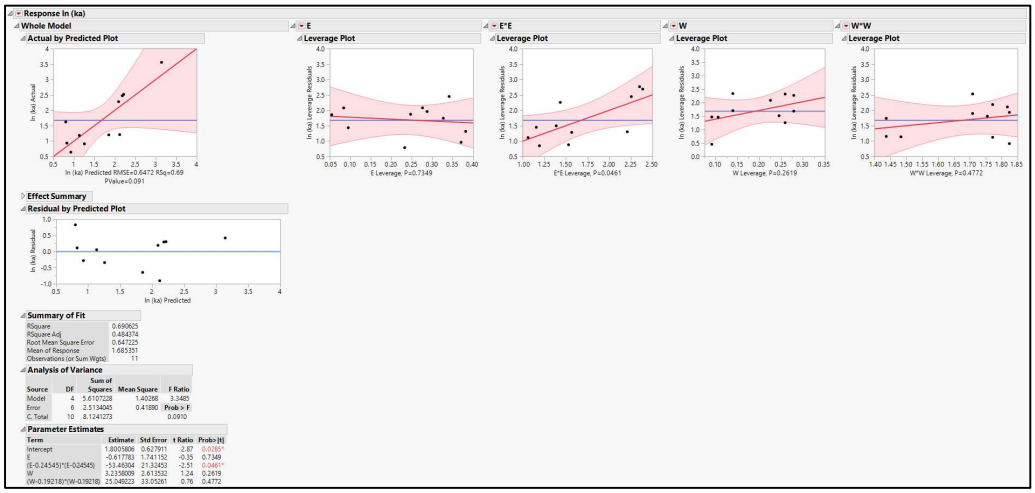

Figure 12: Second Iteration of Extraction Rate Coefficient Model

Response: ln (ka); Factors: E^2, E, W^2, W

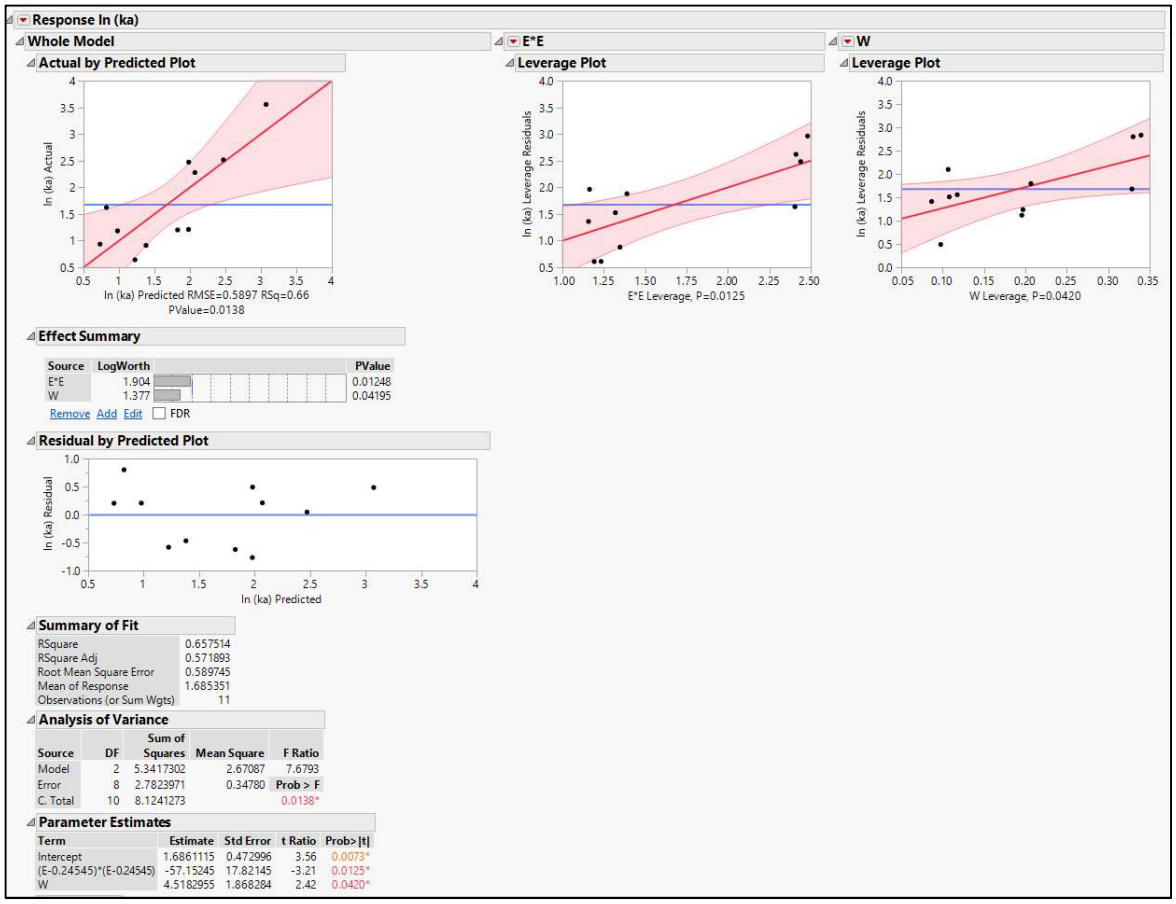

Figure 13: Final Iteration of Extraction Rate Coefficient Model

Response: ln (ka); Factors: E^2, W

CHAPTER II

Calculating the Loading Ratio and the Optimum Extractant Concentration

A version of this chapter will be submitted for publication as a journal article:

DeSimone, D., Counce, R., Watson, J. Calculating the Loading Ratio and Optimum Extractant Concentration for a Solvent Extraction Process. Solvent Extraction and Ion Exchange, 2019.

As lead author of the publication, David DeSimone was responsible for reviewing the literature, designing the experiment, conducting the tests, analyzing the results and writing the journal article. Robert Counce and Jack Watson provided technical expertise and editing guidance. The following chapter focuses on introducing the loading ratio parameter, explaining its need and comparing the theoretical formula to the experimental results. The publication will include all the material below then compare these results to other authors' experimental results.

Abstract

The loading ratio of a solvent extraction process is the ratio of moles of metal extracted to moles of extractant fed. From an economic perspective, it may be beneficial to conduct a process such that the loading ratio is maximized. This could be especially true for processes using costly extractants. With maximizing the loading ratio as a potential process goal, coupled with the Murphree efficiency having specific limitations, it is recommended to quantify systems using the loading ratio in addition to the Murphree efficiency. In this study, the loading ratio is compared to the Murphree efficiency and equations relating the two metrics are presented. It is shown that due to competing effects of the extractant concentration on the loading ratio, an optimum extractant concentration exists for all extraction systems. A procedure to calculate the optimum extractant concentration and the corresponding maximum loading ratio for any extraction system is presented. The procedure is validated by comparing the predicted loading ratios to the actual loading ratios from a previous yttrium-extraction study. Trends suggest that for processes operating below the

optimum extractant concentration, the loading ratio would increase more from increasing the extractant concentration than from increasing the Murphree efficiency. Conversely, for processes operating beyond the optimum extractant concentration, it is recommended to decrease the extractant concentration rather than increasing the Murphree efficiency to significantly increase the loading ratio. Sample calculations for a representative yttrium-extraction system are presented to demonstrate the need to account for the loading ratio during process design. The system operated at 90% efficiency and assumed an extracted metal value equal to six times the extractant cost. Under the given conditions, the system achieved a profit only when operating at the optimum extractant concentration.

Key Words

Loading Ratio, Murphree Efficiency, Extractant Concentration, Optimization, Loading Capacity

Introduction

Historically, the effectiveness of a solvent extraction system has been quantified by the process's Murphree efficiency or extraction rate coefficient [1-3]. However, as discussed below, both the Murphree efficiency and the extraction rate coefficient have significant limitations in thoroughly quantifying an extraction system [4,5]. Loading ratio is an underutilized parameter and is suggested as a standard metric to gauge the effectiveness of a solvent extraction system. Since the Murphree efficiency and the extraction rate coefficient are algebraically coupled (as depicted by equation (17)), the loading ratio is contrasted solely with the Murphree efficiency in the discussion below. In doing so, it is the author's intention to increase awareness of the loading ratio and encourage its use alongside these other metrics.

Although the Murphree efficiency has been widely accepted to define the effectiveness of a solvent extraction process – and it has been used to scale the process to various-sized applications [5] – it has several drawbacks. First, the Murphree efficiency does not provide information regarding the fraction extracted. As equation (8) from the previous chapter shows, the Murphree efficiency is the ratio of the concentration change in a continuous contactor to the concentration change in a corresponding batch test (for a single phase) [2]. In a multi-component system where competition for the extractant exists, or in a single-component system where a low distribution coefficient is observed, a metal may experience a low fraction extracted at equilibrium. Thus, during the continuous process, the contactor could report a high Murphree efficiency even when yielding a low fraction extracted. Therefore, by its definition, the Murphree efficiency may be misleading when quantifying the successfulness of extraction. Secondly, the Murphree efficiency does not indicate the economic viability of the overall process. Since the Murphree efficiency does not account for the material cost, a system with a high Murphree efficiency may still prove to be uneconomical whereas a system with a low Murphree efficiency may prove to be very cost effective. Finally, as previous authors have suggested [4], the Murphree efficiency may not be applicable to all extraction systems.

An alternative parameter is needed to supplement the Murphree efficiency and to account for these limitations. It must indicate the fraction extracted, reference the material costs, and be applicable to all systems. The suggested alternative parameter, loading ratio, fulfills these needs. First, as it is directly proportional to the amount of metal extracted, it gives a clear indication of the fraction extracted. Secondly, since it is inversely proportional to the amount of extractant used, it can easily be employed to estimate the operational costs of the solvent extraction process. Finally, since it is defined as a mole ratio, it inherently accounts for chemical reactions between substances and is therefore applicable to all extraction systems.

Loading ratio, and the related loading capacity, have been used modestly by other authors to classify systems and to quantify results [6-14]. However, there has only been limited

research in formally defining loading ratio and linking it to other well-known parameters [11, 12, 14]. If employed at all, the loading ratio is most often used only to classify the organic-phase streams entering a stripping process (downstream from extraction) [11,15] or to determine the onset of third phase formation [9-11]. However, as is discussed below, the loading ratio should be a targeted metric of the extraction process rather than solely a notated effect of it.

In general, the loading ratio indicates how well a solvent extraction process utilizes its main resource – the extractant. A process operating at the maximum loading ratio uses the extractant most cost effectively. For this reason, it is recommended to target the maximum loading ratio when designing a process. Although it is possible to extract additional metal by operating beyond the maximum loading ratio, doing so necessitates a nonlinear increase in the amount of extractant required. If operating beyond the maximum loading ratio, the benefits of incremental increases in extraction must be weighed against the added costs of larger extractant volumes. If, on the other hand, a process operates at the maximum loading ratio, a large amount of metal is extracted for a minimal amount of extractant.

Approach

In this study, the loading ratio is first formally defined and related to the Murphree efficiency. Next, a procedure is introduced to calculate the maximum loading ratio for any system by determining its optimum extractant concentration. This procedure is used to calculate the theoretical loading ratios for the trials conducted in Chapter I. Then these theoretical values are compared to the Chapter I experimental results to analyze the loading ratio trends and to draw conclusions. Finally, an example process is presented to demonstrate the need to account for the loading ratio during process design.

Results & Discussion

All symbols and nomenclature for the following definitions and derivations are listed in Table 5 in Appendix D. The loading ratio is defined as the moles of metal extracted per mole of extractant fed to the system. Formally this is written as:

$$F \equiv \frac{C_{org\ out} * \frac{1}{m}}{E} \qquad (24)$$

where F is the loading ratio, $C_{org\ out}$ is the metal's mass concentration in the organic phase exiting the contactor, m is the metal's molar mass and E is the extractant molar concentration in the organic-phase feed stream. The maximum value of the numerator of equation (24) is the organic-phase loading capacity. Substituting equation (10) into equation (24) yields:

$$F = \left(\frac{\varepsilon * C_{aq\ in}}{m}\right) * \left(\frac{1}{E}\right) * \left(\frac{D}{1 + D * \frac{\dot{O}}{\dot{A}}}\right) \qquad (25)$$

where ε is the Murphree efficiency, $C_{aq\ in}$ is the metal's mass concentration in the aqueous-phase feed stream, D is the distribution coefficient and $\frac{\dot{O}}{\dot{A}}$ is the organic-to-aqueous flow rate ratio. Equation (25) shows the loading ratio as a nonnegative number that is proportional to the Murphree efficiency and metal concentration in the aqueous-phase feed stream. It is applicable to aqueous-phase continuous systems or organic-phase continuous systems but may experience limitations if phase inversions occur during the process.

The terms in equation (25) are separated into three groups. The first group of terms (Murphree efficiency, aqueous feed-stream concentration and molar mass) is a function of the aqueous-phase feed stream and the process's operational settings. The second group consists of one term – the inverse of the extractant concentration. This term obviously decreases as the extractant concentration increases. The final group, consisting of the distribution coefficient and the flow rate phase ratio, is also a function of the extractant concentration. As the extractant concentration increases, the distribution coefficient

increases. As the distribution coefficient increases, this group of terms will increase and approach the limit of $\frac{\dot{A}}{\dot{O}}$. Therefore, by viewing the loading ratio as a product of these three grouped terms, it is apparent that the extractant concentration yields a competing effect on the loading ratio. The extractant concentration has an inverse effect on the second group, and a direct effect on the third group. From this observation, it can be surmised that an optimum extractant concentration exists and the maximum loading ratio would occur at that concentration. In other words, between an organic-phase molarity of zero (diluent alone) and the greatest molarity possible (pure extractant) there exists an extractant concentration that yields the highest loading ratio. This is true for any metal and any extractant. The location of the optimum varies but its presence can be confirmed.

To determine this optimum extractant concentration and the corresponding maximum loading ratio, the partial derivative of equation (25) is calculated with respect to the extractant concentration. Since the distribution coefficient is a function of the extractant concentration, care must be exercised to ensure that this term is not treated as a constant. Employing both the product and quotient rules yields:

$$\frac{\partial F}{\partial E} = \frac{\varepsilon * C_{aq\ in}}{m} * \left[\frac{\left(\frac{\partial D}{\partial E}\right)}{E * \left(1 + D * \frac{\dot{O}}{\dot{A}}\right)^2} - \frac{D}{E^2 * \left(1 + D * \frac{\dot{O}}{\dot{A}}\right)} \right] \qquad (26)$$

with $\frac{\partial F}{\partial E}$ being the change in loading ratio with respect to the extractant concentration and $\frac{\partial D}{\partial E}$ being the change in the distribution coefficient with respect to the extractant concentration. Equation (26) is applicable to systems with distribution coefficients that behave linearly or nonlinearly with respect to the extractant concentration. By setting the left side of equation (26) to zero and simplifying the result, the extractant concentration yielding the maximum loading ratio is determined as:

$$E = \frac{D * \left(D * \frac{\dot{O}}{\dot{A}} + 1\right)}{\left(\frac{dD}{dE}\right)} \qquad (27)$$

Equation (27) is powerful. It shows that for any extraction system, a maximum loading ratio exists, and the location of that maximum can be calculated knowing only the equilibrium conditions and the flow rate ratio. This equation pertains to systems experiencing either linear or nonlinear equilibrium trends.

Equation (27) is a separable first order ordinary differential equation (ODE) and is solvable via direct integration. By rearranging it as follows, it predicts how the distribution coefficient changes as the extractant concentration changes when operating at the maximum loading ratio:

$$\left(\frac{dD}{dE}\right) = \frac{D * \left(D * \frac{\dot{O}}{\dot{A}} + 1\right)}{E}$$

Since all the terms on the right side of this equation are positive, the left side of this equation will always be positive. This is as expected since increasing the extractant concentration yields an increase in the distribution coefficient. Solving the ODE explicitly for the distribution coefficient yields:

$$D = \frac{B * E}{1 - B * E * \frac{\dot{O}}{\dot{A}}} \qquad (28)$$

where B is a constant of integration and is specific to each extraction process. Equation (28) shows the relationship between the distribution coefficient and the extractant concentration for systems operating at the optimum extractant concentration.

To use equation (27), it is suggested to experimentally determine the distribution coefficient at several extractant concentrations. By doing so, an equilibrium model can be developed to depict the distribution coefficient as a function of the extractant concentration. This model and its derivative would be substituted into equation (27) for D and for $\frac{dD}{dE}$, respectively. By inputting the process flow rate ratio into equation (27) as well, the extractant concentration yielding the maximum loading ratio is determined. This maximum loading ratio can then be calculated via equation (25) by inputting the operational variables, the equation (27)

extractant concentration, and the equilibrium model developed previously. Using the data obtained in Chapter I, an example of this process is detailed below.

It may be possible that two optimum extractant concentrations exist – one within the aqueous-phase continuous regime and one within the organic-phase continuous regime. If the continuous phase of operation is unknown, it is recommended to model the equilibrium conditions at or near the operational parameters. This will ensure the necessary values of D and $\frac{dD}{dE}$ are substituted into equation (27). By doing so, the optimum extractant concentration and maximum loading ratio that apply to the system would be calculated correctly by equations (27) and (25), respectively.

To demonstrate the procedure for a specific process, the results from Chapter I are referenced. The 12 batch tests provided data points for which an equilibrium model could be developed. Table 6 in Appendix D lists the measured distribution coefficient for each trial. Figure 14 in Appendix E depicts a log-log plot of the distribution coefficients versus the extractant concentrations. By fitting a linear regression model to the 12 data points, a relationship was developed to represent the distribution coefficient as a function of the extractant concentration. Figure 15 in Appendix E depicts the development of the resulting mathematical model:

$$D = 110 * E^2 \qquad (29)$$

The first derivative of this modeled equation is:

$$\frac{dD}{dE} = 220 * E \qquad (30)$$

By substituting equations (29) and (30) into equation (27), and inputting the flow rate ratio used during the study (0.1), the optimum extraction concentration is calculated to be 0.3 *M*. Substituting this calculated value for E and substituting equation (29) for D into equation (25) yields the maximum loading ratio as a function of Murphree efficiency. The corresponding process parameters for $C_{aq\ in}$, m and $\frac{\dot{O}}{\dot{A}}$ must also be substituted into equation (25): 1 g/L, 88.9 g/mol and 0.1, respectively. Therefore, assuming a process with a Murphree

efficiency of 100%, the maximum loading ratio for the Chapter I study was calculated to be approximately 0.187 mol Y per mol DEHPA. This maximum loading ratio would occur at the optimum extractant concentration of 0.3 *M*.

Using these Chapter I process parameters, Figure 16 in Appendix E shows a graphical depiction of equation (25). The family of curves represents the projected loading ratio as a function of both the extractant concentration and the Murphree efficiency. Note that the maximum loading ratio for each curve occurs at the extractant concentration of 0.3 *M* (as calculated above). As equation (27) suggests, the location of the maximum is not dependent on the efficiency. The location is, however, dependent on the equilibrium conditions and the flow rate ratio. The Chapter I study was conducted at a single flow rate ratio. However, if the $\frac{\dot{O}}{\dot{A}}$ had decreased, the maximum loading ratio would be greater and would have occurred at a greater extractant concentration (peak shifting up and to the right). Conversely, if the $\frac{\dot{O}}{\dot{A}}$ had increased, the maximum loading ratio would be less and would have occurred at a lower extractant concentration (peak shifting down and to the left).

Using a procedure like the one employed in the previous walkthrough, the projected loading ratio was calculated for each Chapter I trial. In the previous example, the loading ratio at the optimal extractant concentration was determined. However, in this case, the goal is to determine the loading ratio at each trial's actual extractant concentration. First, the distribution coefficient at each extractant concentration was estimated from equation (29). Then, as was done in Chapter I, the Murphree efficiency was calculated via equation (8). These values and the pertinent process conditions were substituted into equation (25) to yield the projected loading ratio for each trial. Finally, these predicted values were compared to the actual loading ratios for each trial. The actual loading ratio was calculated by directly measuring the organic-phase exit stream concentration for each trial and dividing by the extractant concentration. Table 6 lists the predicted and actual loading ratios for each trial

as well as the modeled distribution coefficient and calculated efficiency. Trial 9 was again omitted from analysis since the efficiency was calculated to be greater than 100%.

To test the accuracy of equation (25) in predicting the loading ratio for the 11 valid trials, a plot of the actual loading ratio versus the predicted loading ratio was constructed. Figure 17 in Appendix E shows the actual versus predicted plot for each trial and groups the data according to extractant concentration. In general, the actual values for the loading ratio are approximately equal to the predicted values for the loading ratio. If equation (25) were to predict the loading ratio perfectly, each data point on Figure 17 would fall on the line $y = x$. Although scatter is present, equation (25) predicts the loading ratio for the 11 trials reasonably well (since the points are reasonably well aligned). However, for 9 of the 11 trials (82%), the data fall below the line. This means that equation (25) overestimated the loading ratio for these trials and therefore it may exhibit slight bias. Figure 18 in Appendix E depicts the statistics of the Figure 17 plot. It shows the linear regression trend and the R^2 value associated with Figure 17. Using an alpha value of 0.05, the confidence interval of the trendline slope was (0.69, 1.06) with a point estimate of 0.87. Since the confidence interval encompasses the targeted slope of 1.0, it is inferred that equation (25) is unbiased. The reported R^2 value was 0.93.

The actual loading ratios for the 11 valid trials are plotted against the extractant concentration with iso-efficiency lines added (see Figure 19 in Appendix E). Trials conducted at the same efficiency are connected by an iso-efficiency line to ensure that similar trials are compared during analysis. Two iso-efficiency lines are shown. The first line connects trials 11, 3, and 8 (for extractant concentrations 0.1 *M*, 0.2 *M* and 0.4 *M*, respectively) since these trials operated at 75% efficiency (+/- 2%). The second line connects trials 10, 4, and 5 (for extractant concentrations 0.1 *M*, 0.2 *M* and 0.4 *M*, respectively) since these trials operated at 50% efficiency (+/- 5%). Since no trials were conducted at an extractant concentration of 0.3 *M*, the expected peak at this concentration could not be confirmed. However, Figure 19 still supports the loading ratio trend predicted

by equation (25). As shown on Figure 16, the loading ratios predicted at 0.2 *M* are approximately equal to the loading ratios predicted at 0.4 *M* for a given efficiency. This is especially true at lower efficiencies and is well depicted by the nearly horizontal iso-efficiency lines connecting the 0.2 *M* and the 0.4 *M* trials on Figure 19. By visualizing the data in this manner, it is apparent that the actual loading ratios pass through a maximum value between extractant concentrations of 0.1 *M* and 0.4 *M*.

Using the iso-efficiency lines, Figure 19 demonstrates how similar efficiencies may yield different loading ratios. Trial 11 (square data point) operated at 75% efficiency, but its measured loading ratio was only half of the calculated maximum loading ratio (F_{max} = 0.187 mol Y per mol DEHPA, as calculated above). In contrast, trial 3 (circle data point) also operated at 75% efficiency but obtained nearly two-thirds of the calculated maximum loading ratio. This shows that the loading ratio increased as the extractant concentration increased for trials conducted below the optimum extractant concentration and at equal efficiencies. This same trend was observed when comparing trials 10 and 4 at 50% efficiency (square data point and circle data point, respectively). It suggests that when operating below the optimum extractant concentration, it may be more economical to increase the extractant concentration and maintain the process efficiency rather than increase the process efficiency and maintain the extractant concentration. This effect is attributed to the third group of terms in equation (25). At extractant concentrations below the optimum, the effect of the third group controls the loading ratio.

This trend does not continue for extractant concentrations above the optimum. At high extractant concentrations, the effect of the second group of terms in equation (25) controls the loading ratio. As seen in Figure 19, the data depict this relationship as well. At 75% efficiency, trial 3 (circle data point) and trial 8 (triangle data point) yielded the same approximate loading ratio (0.12 mol Y/mol DEHPA). Here, increasing the extractant concentration (and therefore increasing the organic-phase cost) could result in limited, if any, potential economic gain. Although more metal is extracted by increasing the extractant

concentration, it is done at a greater cost. Again, the same trend holds when comparing trials 4 and 5 at 50% efficiency (circle data point and triangle data point, respectively). For these trials, there would be an increase in organic-phase cost without an increase in the loading ratio. For costly extractants, this might decrease the economic viability of the process. Therefore, if operating beyond the optimum extractant concentration, it may be beneficial to decrease the extractant concentration and operate at the same process efficiency.

Finally, to illustrate the need to consider the loading ratio during process design, Tables 7A and 7B in Appendix D present an example solvent extraction process. This representative example serves only to illustrate the need to consider the loading ratio and may not reflect actual costs. Likewise, it does not consider additional unit operations such as stripping that would affect results. However, for the solvent extraction process described, it is evident that the loading ratio plays a significant role in process economics and should be considered for all processes. Sample calculations have been presented for four scenarios in a scaled-up process employing the same flow rate ratio, aqueous-phase feed stream concentration and distribution coefficient model as the yttrium-extraction process described earlier. The four scenarios correspond to four potential extractant concentrations: 0.1 *M*, 0.2 *M*, 0.3 *M*, 0.4 *M*. By assuming a 90% Murphree efficiency and valuing the extracted yttrium at six times the cost of the extractant, the projected profit over an 8-hour period was calculated for each scenario. For the given parameters, the only scenario that proved to be profitable was the process operating at the optimum extractant concentration (0.3 *M*). The processes using lower extractant concentrations did not extract enough yttrium whereas the process using a higher extractant concentration did not overcome the extractant costs. The assumed process parameters affected the projected values, but the overall trend remained constant when the yttrium value was six times the extractant cost. Therefore, although many factors affect process economics, the loading ratio should be used as a metric to gauge extraction success and the optimum extractant concentration should be considered during process design.

Conclusion

It has been shown that all solvent extraction processes have an optimum extraction concentration corresponding to a maximum loading ratio. To utilize the extractant most effectively, it is recommended to operate at this optimum extractant concentration and to target the maximum loading ratio. Use of additional extractant beyond the optimum may decrease the economic viability of the extraction process – especially for costly extractants. Equations relating the loading ratio to the Murphree efficiency have been presented and the limitations of solely using the Murphree efficiency have been discussed. A procedure was introduced to calculate the optimum extractant concentration and to predict the loading ratio for any solvent extraction system. The validity of the procedure was confirmed by accurately predicting the actual loading ratios for a previous yttrium-extraction study. Sample calculations were provided to indicate the need to consider a high loading ratio as a targeted metric during process design. It was realized that to achieve a higher loading ratio, operating nearer to the optimum extractant concentration is more effective than increasing the process efficiency.

References

1. Ryon, A.D. and R.S. Lowrie, Experimental basis for the design of mixer settlers for the Amex solvent extraction process. 1963.
2. Treybal, R.E., Liquid Extraction. 2nd ed. Chemical Engineering, ed. M. Peters. 1963, New York: McGraw-Hill. 621.
3. Aly, G.W., B., Dynamic Behaviour of Mixer-Settlers: II. Mathematical Models and Identification Methods. J. Applied Chemical Biotechnology, 1972. 22: p. 1165-1184.
4. Gonda, K.M., S.; Fukuda, S., Stage Efficiency for Mixer-Settlers Process with Chemical Reactions. Journal of Nuclear Science and Technology, 1986. 23(3): p. 279-281.
5. Stevens, G.W.P., H.R.C., Solvent Extraction Equipment Design and Operation: Future Directions from and Engineering Perspective. Solvent Extraction and Ion Exchange, 2000. 18(6): p. 1051-1078.
6. Hino, A.N., S.; Hirai, T.; Komasawa, I., Practical Study of Liquid-Liquid Extraction Process for Separation of Rare Earth Elements with Bis(2-Ethylhexyl) Phosphinic Acid. Journal of Chemical Engineering of Japan, 1997. 30: p. 1040-1046.
7. Nishihama, S.H., A.; Hirai, T.; Komasawa, I., Extraction and Separation of Gallium and Indium from Aqueous Chloride Solution Using Several Organophosphorus Compounds as Extractants. Journal of Chemical Engineering of Japan, 1998. 31(5): p. 818-827.
8. Kim, B.S.H., Y.K.; Huh, Y.S.; Hong, W. H., Predispersed Solvent Extraction of Succinic Acid Aqueous Solution by Colloidal Liquid Aphrons in Column. Biotechnology and Bioprocess Engineering, 2004. 9: p. 454-458.
9. Suresh, A.S., N.L.; Selvan, R.; Antony, M.P.; Srinivasan, T.G., Extraction of U(VI) by Tri-n-Amyl Phosphate Under High Solvent Loading Conditions. Nuclear Technology, 2009. 167: p. 333-338.
10. Tachimori, S.S., Yuji; Suzuki, Shin-ichi, Modification of TODGA - n - dodecane Solvent with a Monoamide for High Loading of Lanthanides(III) and Actinides(III). Solvent Extraction and Ion Exchange, 2002. 20(6): p. 687-699.

11. Morita, Y., Development of a New Extractant and a New Extraction Process for Minor Actinide Separation, in IOP Conference Series: Materials Science and Engineering. 2010, IOP Publishing.
12. Natarajan, R.D., K. Sharma, P.K.; Pugazhendi, S.; Vijayakumar, V.; Pandey, N. K.; Subba Rao, R. V., Optimization of Flowsheet for Scrubbing of Ruthenium during the Reprocessing of Fast Reactor Spent Fuels. Separation Science and Technology, 2013. 48: p. 2494-2498.
13. Tsutsui, N.B., Y.; Sagawa, H.; Ishii, S.; Matsumura, T., Solvent Extraction of Uranium with N,N-Di(2-Ethylhexyl) Octanamide from Nitric Acid Medium. Solvent Extraction and Ion Exchange, 2017. 35(6): p. 439-449.
14. Watari, T.T., D.; Nishihama, S.; Yoshizuka, K., Separation of Cobalt and Nickel with 2-Ethylhexyl Phosphonic Acid Mono-2-Ethylhexyl Ester Using a Countercurrent Mixer-Settler Cascade. Solvent Extraction Research and Development, Japan, 2017. 24(2): p. 131-140.
15. Olivier, M.C.D., C.; Eksteen, J.J., Evaluating a Solvent Extraction Process Route Incorporating Nickel Preloading of Cyanex 272 for teh Removal of Cobalt and Iron from Nickel Sulphate Solutions. Minerals Engineering, 2012. 27-28: p. 37-51.

Appendix D

Table 5: Chapter II Symbols, Notation and Units

Symbol	Definition	Units
$\dot{A}$	Volumetric Flow Rate of Aqueous-Phase Feed Stream	$\frac{L_{aq}}{min}$
B	Integration Constant	$\frac{L_{aq}}{mol_{extractant}}$
$C_{aq\ in}$	Metal Concentration in Aqueous Phase Entering System	$\frac{g_{metal}}{L_{aq}}$
$C_{org\ out}$	Metal Concentration in Organic Phase Exiting System	$\frac{g_{metal}}{L_{org}}$
D	Distribution Coefficient	$\frac{L_{aq}}{L_{org}}$
E	Extractant Concentration	$\frac{mol_{extractant}}{L_{org}}$
F	Organic-Phase Loading Ratio	$\frac{mol_{metal}}{mol_{extractant}}$
m	Metal Molar Mass	$\frac{g_{metal}}{mol_{metal}}$
$\dot{O}$	Volumetric Flow Rate of Organic-Phase Feed Stream	$\frac{L_{org}}{min}$
$\frac{\partial D}{\partial E}$	Change in Distribution Coefficient w.r.t. Extractant Concentration	$\frac{L_{aq}}{mol_{extractant}}$
$\frac{\partial F}{\partial E}$	Change in Loading Ratio w.r.t. Extractant Concentration	$\frac{\left(\frac{mol_{metal}}{mol_{extractant}}\right)}{\left(\frac{mol_{extractant}}{L_{org}}\right)}$
ε	Murphree Efficiency	-

Table 6: Trial Results Grouped by Increasing Extractant Concentration

Trial #	E	D (actual)	D (eqn 29)	ε (eqn 8)	F (eqn 25)	F (actual)
9	0.10	1.30	1.1	~~1.12~~	~~0.125~~	~~0.133~~
10	0.10	1.59	1.1	0.45	0.050	0.046
12	0.10	0.98	1.1	0.38	0.042	0.044
11	0.10	1.06	1.1	0.75	0.084	0.095
4	0.20	4.12	4.4	0.50	0.086	0.078
3	0.20	3.89	4.4	0.75	0.129	0.119
2	0.20	3.53	4.4	0.79	0.136	0.132
1	0.20	3.26	4.4	0.91	0.156	0.149
7	0.40	15.42	17.6	0.62	0.111	0.097
8	0.40	23.59	17.6	0.77	0.138	0.115
5	0.40	18.23	17.6	0.55	0.099	0.077
6	0.40	21.67	17.6	0.69	0.124	0.109

Table 7A: Operational Parameters for Four Example Process Scenarios

Basis	min	480
Org Flow Rate	Lorg / min	4.55
Aq Flow Rate	Laq / min	45.5
O:A	Lorg / Laq	0.1
Caq in	gY / Lorg	1
Y Molar Mass	gY / mol Y	88.9
Extractant Cost	$ / mol ext	40
Yttrium Value	$ / mol Y	240
Efficiency	-	0.9

Table 7B: Projected Outcomes for Four Example Process Scenarios

Extractant Concentration	Amount of Extractant Used	Cost of Extractant	D	Corg out	Amount of Y Extracted	Value of Y Extracted	Profit	Loading Ratio
mol ext / Lorg	mol ext	$	Laq / Lorg	gY / Lorg	mol Y	$	$	mol Y / mol ext
0.1	218.4	$8,736	1.1	0.89	21.91	$5,259	-$3,477	0.100
0.2	436.8	$17,472	4.4	2.75	67.56	$16,214	-$1,258	0.155
0.3	655.2	$26,208	9.9	4.48	110.00	$26,399	$191	0.168
0.4	873.6	$34,944	17.6	5.74	140.99	$33,838	-$1,106	0.161

Appendix E

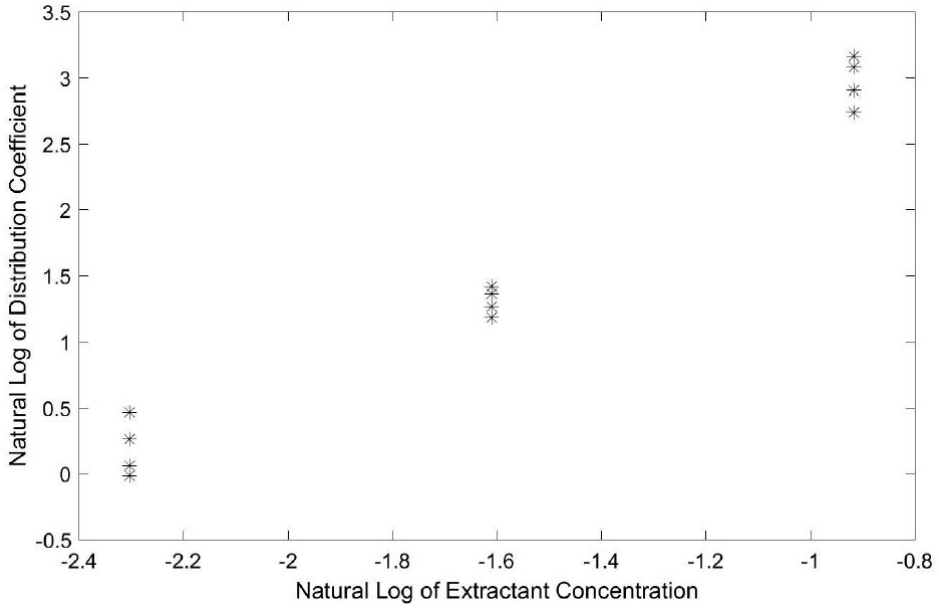

Figure 14: Effect of the Extractant Concentration on the Distribution Coefficient for Yttrium Extraction by DEHPA

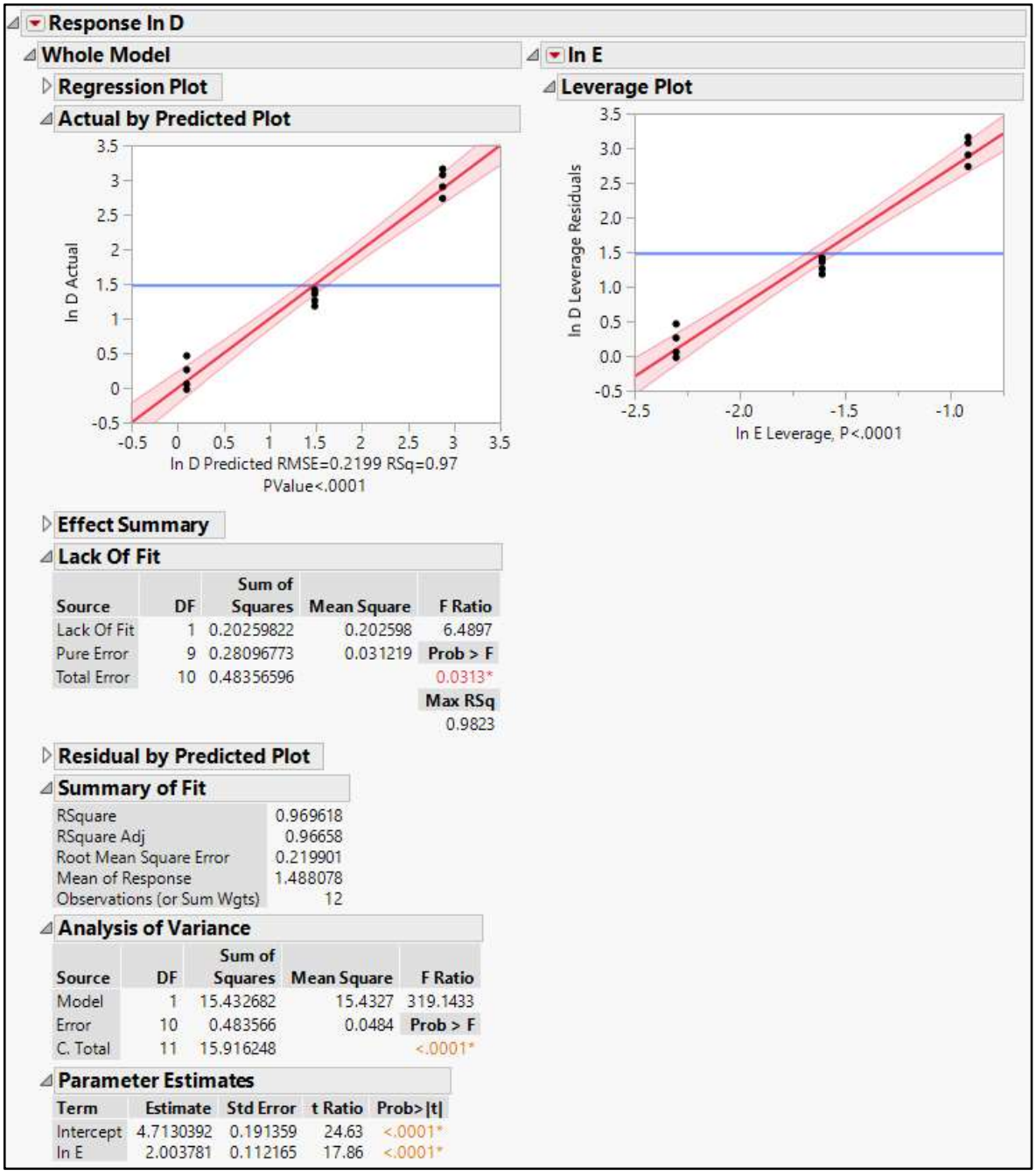

Figure 15: Model of Distribution Coefficient as Function of Extractant Concentration for Yttrium Extraction by DEHPA

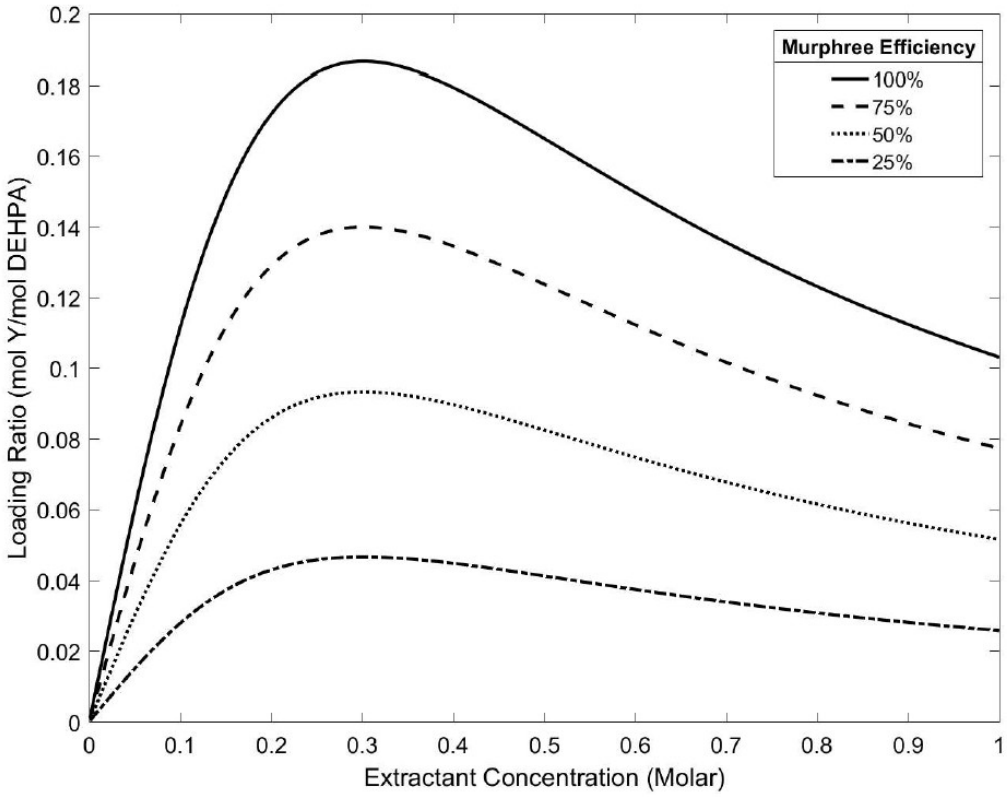

Figure 16: Visualization of Equation (25) for Yttrium Extraction by DEHPA

$$C_{aq\ in} = 1.0\frac{g\ Y}{L};\ \frac{\dot{O}}{\dot{A}} = 0.1; D = 110E^2$$

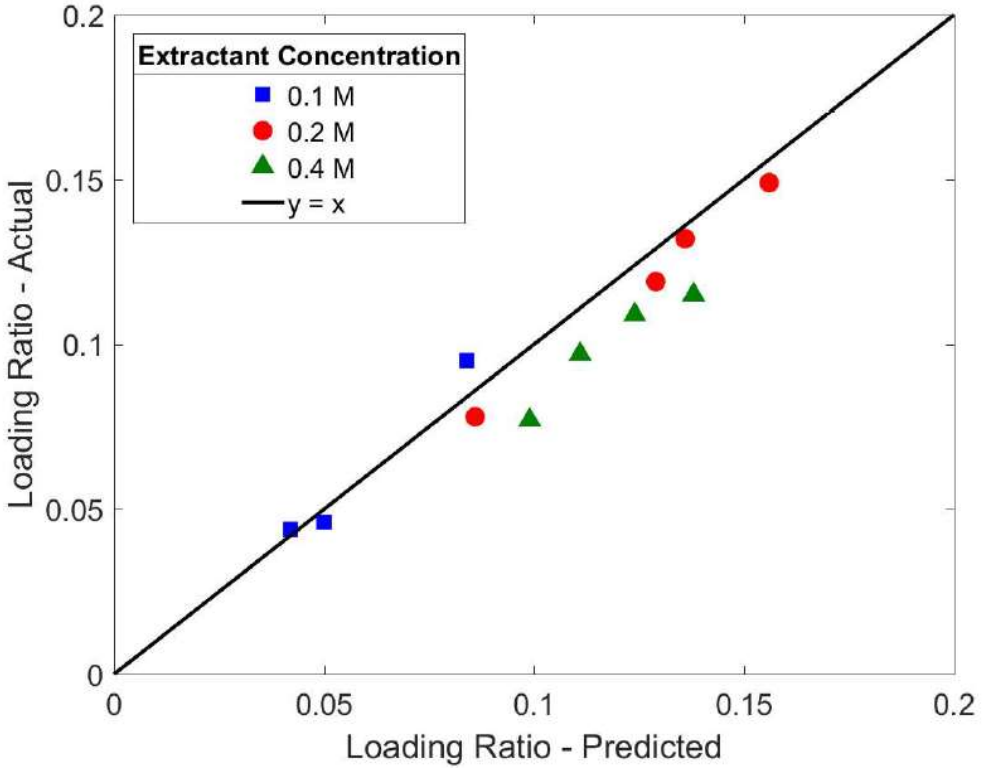

Figure 17: Loading Ratio for Yttrium Extraction by DEHPA – Actual vs. Predicted Grouped by Extractant Concentration

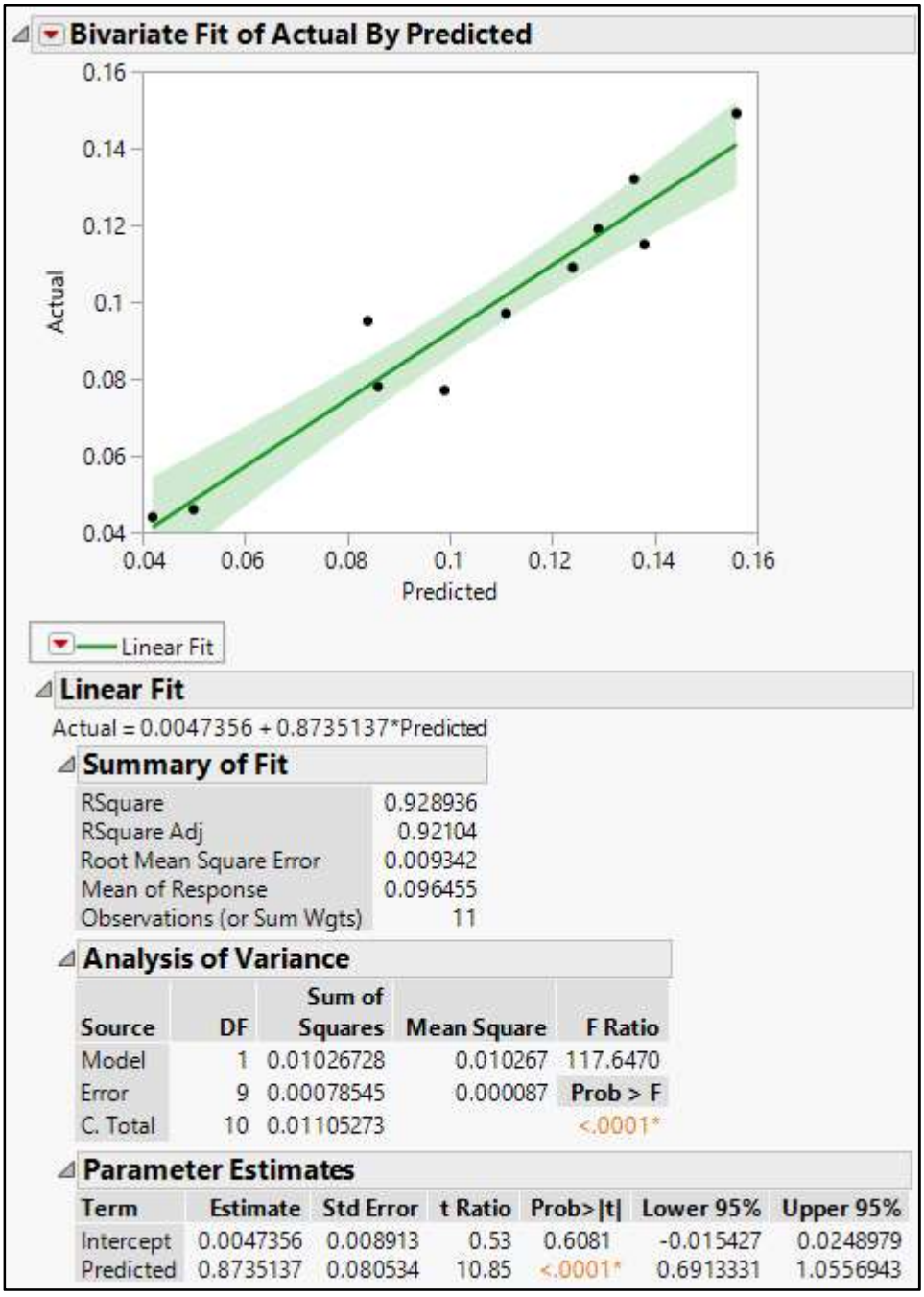

Figure 18: Loading Ratio for Yttrium Extraction by DEHPA – Actual vs. Predicted Trend Statistics

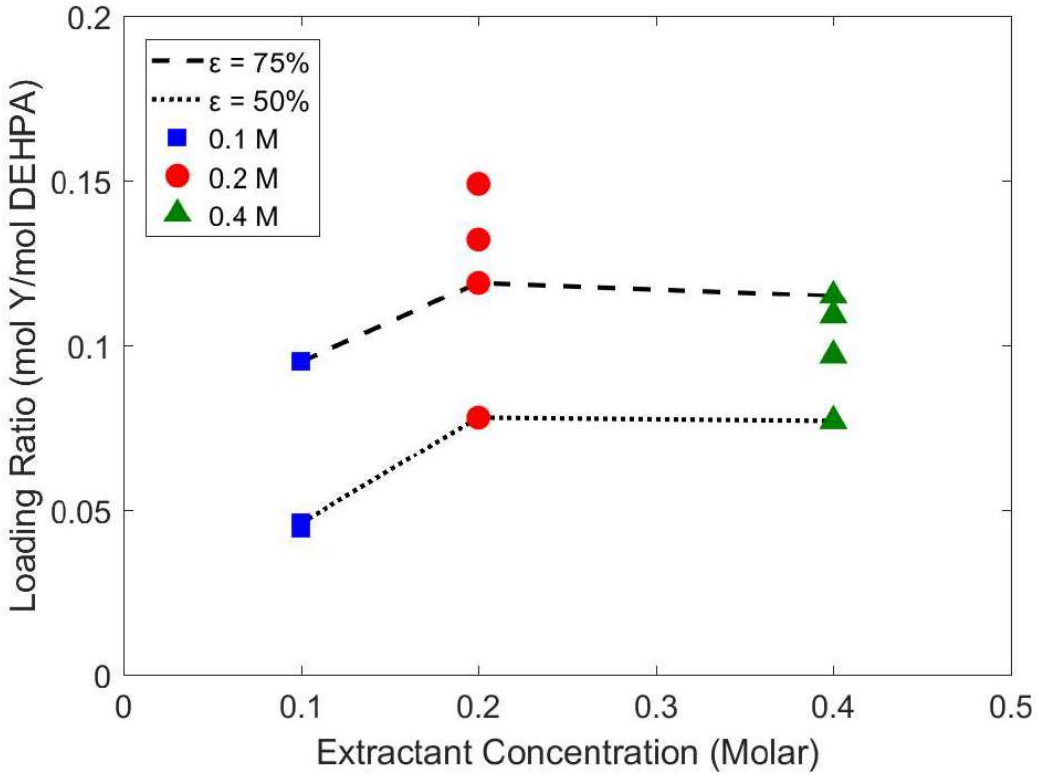

Figure 19: Loading Ratio vs. Extractant Concentration for Yttrium Extraction by DEHPA – Measured Results with Iso-Efficiency Lines

CHAPTER III

Modeling the Stoichiometric Ratio for Yttrium Extraction from Hydrochloric Acid

A version of this chapter will be submitted for publication as a journal article:

Ghezawi, N., DeSimone, D., Counce, R., Watson, J. Activity Coefficients of Yttrium Chloride Solutions. Solvent Extraction and Ion Exchange, 2019.

The manuscript below is a static instance of a working document. The detailed experimental background, references, and validations are not included in the draft below. As secondary author of the publication, David DeSimone was responsible for analyzing the data and interpreting the results. Natasha Ghezawi reviewed the literature and conducted the experiments. Robert Counce and Jack Watson provided technical expertise and editing guidance. The following chapter focuses on data analysis and interpretation to determine the stoichiometric ratio for the given system. The publication will include all the material below plus a thorough literature review and introduction. It will also compare the model developed herein to experimental results obtained by other authors.

Abstract

Equilibrium conditions for the extraction of yttrium from hydrochloric acid using di(2-ethylhexyl) phosphate (DEHPA) were explored. Since chloride molecules had complexed with yttrium ions and had extracted into the organic phase, the equilibrium conditions were described using two simultaneous equilibrium equations. The resulting stoichiometric ratio was lower than the theoretical value of 3. A designed experiment was conducted to determine the effects of the O:A, the aqueous-phase hydrogen ion concentration before contact and the aqueous-phase yttrium ion concentration before contact on the actual stoichiometric ratio. Since the O:A was deemed not significant, a model predicting the actual stoichiometric ratio as a function of the hydrogen ion concentration and the yttrium ion concentration before contact is presented. Use of the aqueous-phase activity coefficients to increase precision was explored but deemed unnecessary. In general, increasing the aqueous-phase hydrogen ion concentration yielded a decrease in the stoichiometric ratio.

This indicated that additional chloride molecules were extracted into the organic phase when using concentrated hydrochloric acid. Increasing the aqueous-phase yttrium ion concentration yielded a similar effect but to a lesser degree.

Key Words

Stoichiometric Ratio, Activity Coefficient, Equilibrium Constant, Yttrium, Complexation

Introduction

All symbols and nomenclature for the following definitions and derivations are listed in Table 8 in Appendix F. It has been shown that the extraction of metal from acidic media does not necessarily follow the stoichiometric ratio predicted by the metal's presumed valence charge. Therefore, for the process used herein, the extraction equilibrium should be written as:

$$Y^{n+} + n \cdot \overline{H_2X_2} \leftrightarrow \overline{Y(HX_2)_n} + n \cdot H^+ \qquad (31)$$

where n is the overall stoichiometric ratio for the extraction, H_2X_2 refers to the dimeric form of DEHPA and the overbars indicate the species resides in the organic phase. Although n is often assumed to be 3 for yttrium extraction, previous studies have shown that actual yttrium extraction yields stoichiometric ratios between two and three. However, rarely have other authors given quantitative explanations for this deviation from ideality. It will be shown not only that the stoichiometric ratio is less than three, but also that this deviation from ideality is attributed to chloride complexation. Thus, equation (31) is modeled as a weighted combination of two simultaneous equilibrium extraction equations. The first equation employs a stoichiometric ratio of 3 and the second equation employs a stoichiometric ratio of 2, as shown below:

$$Y^{3+} + 3\overline{H_2X_2} \leftrightarrow \overline{Y(HX_2)_3} + 3H^+ \qquad (32)$$

$$(YCl)^{2+} + 2\overline{H_2X_2} \leftrightarrow \overline{YCl(HX_2)_2} + 2H^+ \qquad (33)$$

where $(YCl)^{2+}$ refers to the yttrium-chloride complex and $YCl(HX_2)_2$ refers to the yttrium-chloride-extractant complex. To employ an equation with a stoichiometric ratio of 2 and for that equation to maintain net ionic neutrality, it was assumed that a chloride ion was bound to the yttrium ion during extraction. Therefore, equation (33) depicts the yttrium-chloride complex reacting with the extractant at the aqueous-organic interface and allowing a chloride molecule to enter the organic phase. This assumption was validated during experimentation.

The equilibrium constants for equations (32) and (33) can be calculated via one of two methods. Method A is a streamlined method that does not employ aqueous-phase activity coefficients as correction factors whereas method B uses the aqueous-phase activity coefficients to produce equilibrium constants with higher precision. The equilibrium constant for equation (32) is thus calculated via method A as:

$$K_{1A} = \frac{[\overline{Y(HX_2)_3}]}{[Y^{3+}]} * \frac{[H^+]^3}{[\overline{H_2X_2}]^3} \qquad (34)$$

Taking the natural logarithm of equation (34) yields:

$$\ln K_{1A} = \ln[\overline{Y(HX_2)_3}] + 3\ln[H^+] - \ln[Y^{3+}] - 3\ln[\overline{H_2X_2}] \qquad (35)$$

Likewise, the equilibrium constant for equation (32) is calculated via method B as:

$$K_{1B} = \frac{[\overline{Y(HX_2)_3}]}{\gamma_2[Y^{3+}]} * \frac{{\gamma_1}^3\,[H^+]^3}{[\overline{H_2X_2}]^3} \qquad (36)$$

where $\gamma_1$and γ_2 are the activity coefficients for the hydrogen ion and the yttrium ion, respectively. The natural logarithm of equation (36) is:

$$\ln K_{1B} = \ln[\overline{Y(HX_2)_3}] + 3\ln\gamma_1 + 3\ln[H^+] - \ln\gamma_2 - \ln[Y^{3+}] - 3\ln[\overline{H_2X_2}] \qquad (37)$$

Similarly, the equilibrium constant of equation (33) is calculated via method A as:

$$K_{2A} = \frac{[\overline{YCl(HX_2)_2}]}{[YCl^{2+}]} * \frac{[H^+]^2}{[\overline{H_2X_2}]^2} \qquad (38)$$

The natural logarithm of equation (38) is:

$$\ln K_{2A} = \ln[\overline{YCl(HX_2)_2}] + 2\ln[H^+] - \ln[YCl^{2+}] - 2\ln[\overline{H_2X_2}] \qquad (39)$$

Finally, the equilibrium constant for equation (33) is calculated via method B as:

$$K_{2B} = \frac{\left[\overline{YCl(HX_2)_2}\right]}{\gamma_3[YCl^{2+}]} * \frac{{\gamma_1}^2\,[H^+]^2}{[\overline{H_2X_2}]^2} \qquad (40)$$

where γ_3 refers to the activity coefficient for the yttrium-chloride complex ion. The natural logarithm of equation (40) is:

$$\ln K_{2B} = \ln\left[\overline{YCl(HX_2)_2}\right] + 2\ln\gamma_1 + 2\ln[H^+] - \ln\gamma_3 - \ln[YCl^{2+}] - 2\ln[\overline{H_2X_2}] \qquad (41)$$

By experimentally determining the values for each of the right-hand side parameters in equations (35), (37), (39), and (41), the equilibrium constants were modeled as functions of the extraction's initial conditions. Models were developed for both method A and method B to determine if the added precision of method B was warranted. Then, by using these models, the overall stoichiometric ratio was predicted over the experimental range for a given set of initial conditions.

Approach

A previous exploratory study was conducted where the aqueous-phase initial hydrogen ion concentration, aqueous-phase initial yttrium ion concentration, and organic-phase initial extractant concentration were varied in a 3-factor, 12-treatment designed experiment. Preliminary results of the exploratory study indicated that the extractant concentration did not significantly affect the equilibrium constant over the given experimental range. Therefore, for this follow-up study, equilibrium extractions were conducted where the aqueous-phase initial hydrogen ion concentration, aqueous-phase initial yttrium ion concentration and organic to aqueous phase ratio (O:A) were varied. Initial concentrations refer to concentrations before equilibrium contact whereas all equilibrium concentrations are measured after equilibrium contact. A designed experiment was proposed where the hydrogen ion concentration ranged from 0.1 *M* to 0.5 *M*, the yttrium ion concentration varied from 0.25 g/L to 1.25 g/L and the O:A varied from 0.1 to 1.0. These three factors were systematically varied over their respective ranges to yield the follow-up 12-trial designed experiment. One center-point treatment was replicated. One treatment was conducted at the exploratory study's O:A. The initial hydrogen ion concentration was varied by varying the

hydrochloric acid concentration of the aqueous phase. The initial yttrium ion concentration was varied by varying the concentration of yttrium chloride compound dissolved in the aqueous phase. Each trial was conducted such that the aqueous and organic phases were gently rotated for five minutes to reach equilibrium. The equilibrium concentration for each specie was measured for each trial. The equilibrium constants were calculated for each trial by substituting these measured concentrations into equations (35), (37), (39), and (41). Aqueous-phase activity coefficients were calculated for equations (37) and (41) via the modified Pitzer equation. Hydrogen ion concentrations were calculated via titration. Chloride concentrations were calculated via Volhard titrations and quantitative reactions using silver nitrate. The latter process confirmed that the chloride molecule had complexed with the yttrium ion to enter the organic phase. Yttrium ion concentrations were calculated via ICP-OES. Unreacted extractant concentrations were calculated via mass balance.

Results

Table 9 in Appendix F shows the levels for each factor and the corresponding results of the designed experiment. Natural logarithms of K_{1A}, K_{1B}, K_{2A}, and K_{2B} were calculated for each trial. Based on the results of the exploratory study, trial 5 was omitted from this analysis. Conditions similar to those of trial 5 had been tested in quadruplicate during the exploratory study and all four tests yielded concentrations comparable to each other. However, these results were vastly different from those of trial 5 and therefore trial 5 was omitted from analysis. The resulting experimental O:A range was 0.55 to 1.00.

Using the remaining 11 trials, a linear least square regression analysis was conducted for each equilibrium constant. The natural logarithm of the equilibrium constant was the response variable while the initial hydrogen ion concentration, initial yttrium concentration and O:A were the factor variables. Trial 1 was an extreme outlier for every model and thus removed. Each equilibrium constant was then modeled again without trial 1. The O:A was not significant in any model and thus removed as a factor. Ultimately, the natural logarithm

of each equilibrium constant was thus modeled as a function of the initial hydrogen ion concentration and initial yttrium ion concentration. The four final models of the natural logarithms of K_{1A}, K_{1B}, K_{2A}, and K_{2B} are depicted in Figures 20, 21, 22 and 23, respectively in Appendix G.

Discussion

The appropriate method (A or B) for calculating the equilibrium constant was first studied. By comparing Figure 20 to Figure 21, and Figure 22 to Figure 23, it can be seen that adding the aqueous-phase activity coefficients increased the model precision. For both K_1 and K_2, the R^2 value increased from method A to method B. For K_1, the R^2 value increased from 0.79 to 0.86 whereas for K_2 it increased from 0.96 to 0.97. This indicated that more of the variation in the response was explained by adding the activity coefficients. However, this added precision came with multiple costs. First, the model complexity increased. Models with less complexity are often favored because they do not overparameterize a system. Adding the two activity coefficients to the streamlined model may have made it applicable to fewer systems. Also, there was a computational cost in determining the activity coefficients. The streamlined model maintains the advantage of requiring fewer input parameters and therefore can be applied more easily without additional calculations. Since the R^2 value increased by only 0.07 for K_1 and 0.01 for K_2, it is recommended to use the model without the activity coefficients for ubiquity, clarity and simplicity. Therefore, for the remainder of the discussion, method A (equating to equilibrium constants K_{1A} and K_{2A}) is employed. The resulting models for the natural logarithms of the equilibrium constants are:

$$\ln K_{1A} = -21.3x - 5.7y + 12.2 \qquad (42)$$

$$\ln K_{2A} = -11.3x - 5.3y + 6.3 \qquad (43)$$

where x is the initial aqueous-phase hydrogen ion concentration and y is the initial aqueous-phase yttrium ion concentration.

To calculate the overall stoichiometric ratio for equation (31), the actual equilibrium conditions were treated as a weighted average of equation (32) and equation (33). To do so, the ratio of the extraction occurring via equation (32) to the total extraction occurring via either equation (32) or (33) was determined. This value represented the proportion of extraction occurring via equation (32). Therefore, the parameter z was formally defined as:

$$z \equiv \frac{K_1}{K_1 + K_2} \qquad (44)$$

where z is the ratio of extraction taking place via equation (32) to all extraction taking place. If all extraction took place via equation (32), K_2 would equal zero and z would equal 1. Conversely, if all extraction took place via equation (33), K_1 would equal zero and z would equal 0. Thus, since all extraction took place via equation (32) or (33), the stoichiometric ratio was calculated in terms of z as:

$$n = 3z + 2(1 - z) = 2 + z \qquad (45)$$

Substituting the modeled equilibrium constant values from equations (42) and (43) into equation (44) yields an expression for z in terms of the initial ion concentrations. Substituting this expression for z into equation (45) yields:

$$n = 2 + \frac{exp^{-21.3x-5.7y+12.2}}{exp^{-21.3x-5.7y+12.2} + exp^{-11.3x-5.3y+6.3}} \qquad (46)$$

Equation (46) predicts the stoichiometric ratio for equation (31) over the experimental range of initial conditions. For visualization purposes, Figure 24 in Appendix G depicts n as a function of both initial hydrogen ion concentration and initial yttrium concentration. It is apparent that the stoichiometric ratio begins to decrease significantly as the initial acid concentration increases. In other words, when the extraction is conducted with a high molar hydrochloric acid, the equilibrium favors equation (33) over equation (32) and the concentration of chloride molecules entering the organic phase increases. The stoichiometric ratio also decreased as the yttrium concentration increased, but this factor yielded a smaller effect. More yttrium ions were available for complexation at high yttrium concentrations than at low yttrium concentrations. This greater availability most likely led to a greater amount of chloride ions complexing and entering the organic phase.

For completeness, n was also calculated using method B. In doing so, the original approach was validated. There was no significant difference between n calculated via method A and via method B for moderate concentrations. It is therefore not necessary to account for the aqueous-phase activity coefficients when calculating the equilibrium constants for this system. Figure 25 in Appendix G depicts the stoichiometric ratios calculated using method B. The equation is depicted below:

$$n_B = 2 + \frac{exp^{-2\ .9x-6.1y+15.4}}{exp^{-27.9x-6.1y+15.4} + exp^{-14.7x-5.5y+7.9}} \qquad (47)$$

As Figure 25 depicts, the activity coefficients only become necessary when the yttrium ion concentration or the hydrogen ion concentration increases beyond practical extraction limits.

Conclusion

Solvent extraction of yttrium from hydrochloric acid was studied at equilibrium. In doing so, it was confirmed that chloride molecules enter the organic phase via complexation with yttrium ions. This phenomenon required the equilibrium conditions to be described by a weighted average of two simultaneous extraction equations. By doing so, the stoichiometric ratio could be characterized as a function of the two equilibrium constants. A designed experiment was conducted to model the stoichiometric ratio in terms of the initial conditions (conditions before equilibrium contact). The stoichiometric ratio was thus predicted for the range of experimental conditions. It was determined that the aqueous-phase activity coefficients add minimal precision to the estimates of the equilibrium coefficients and therefore add little to the estimates of the stoichiometric ratio. It is recommended to describe the system without employing activity coefficients to minimize model parameters. Overall, it was determined that increasing the aqueous-phase hydrogen ion concentration yielded additional chloride molecules in the organic phase. Increasing the aqueous-phase yttrium ion concentration yielded a similar effect but to a lesser degree. The O:A yielded a negligible effect on the equilibrium constant and therefore no effect on the stoichiometric ratio.

Appendix F

Table 8: Chapter III Symbols, Notation and Units

Symbol	Definition	Units
K_{1A}	Equilibrium Constant for Reaction 1 Calculated via Method A	-
K_{1B}	Equilibrium Constant for Reaction 1 Calculated via Method B	-
K_{2A}	Equilibrium Constant for Reaction 2 Calculated via Method A	-
K_{2B}	Equilibrium Constant for Reaction 2 Calculated via Method B	-
n	Stoichiometric Coefficient	-
O:A	Organic to Aqueous Phase Ratio	-
x	Initial Aqueous-Phase $[H^+]$	*M*
y	Initial Aqueous-Phase $[Y^{3+}]$	g/L
z	Proportion of Extraction Explained by K_1	-

Table 9: Trial Results Grouped by Increasing [H^+] Concentration

Trial #	[H^+]	[Y^{3+}]	O:A	ln K_{1A} Eqn (35)	ln K_{1B} Eqn (37)	ln K_{2A} Eqn (39)	ln K_{2B} Eqn (41)
~~1~~	~~0.10~~	~~0.25~~	~~1.00~~	~~-2.51~~	~~-0.81~~	~~-2.12~~	~~-1.27~~
2	0.10	0.75	0.55	5.31	7.10	0.56	1.44
3	0.10	1.25	1.00	4.53	6.36	-0.90	-0.01
4	0.30	0.25	0.55	3.56	4.73	1.66	2.24
~~5~~	~~0.30~~	~~0.75~~	~~0.10~~	~~0.35~~	~~1.39~~	~~-4.27~~	~~-3.77~~
6	0.30	0.75	0.55	3.64	4.68	-0.54	-0.04
7	0.30	0.75	0.55	-1.19	-0.14	-0.92	-0.42
8	0.30	0.75	1.00	2.94	3.98	-0.74	-0.24
9	0.30	1.25	0.55	-3.33	-2.42	-4.35	-3.94
10	0.50	0.25	1.00	-0.17	-0.62	-0.64	-0.87
11	0.50	0.75	0.55	-0.53	-1.20	-3.64	-4.00
12	0.50	1.25	1.00	-6.31	-7.20	-5.73	-6.22

APPENDIX G

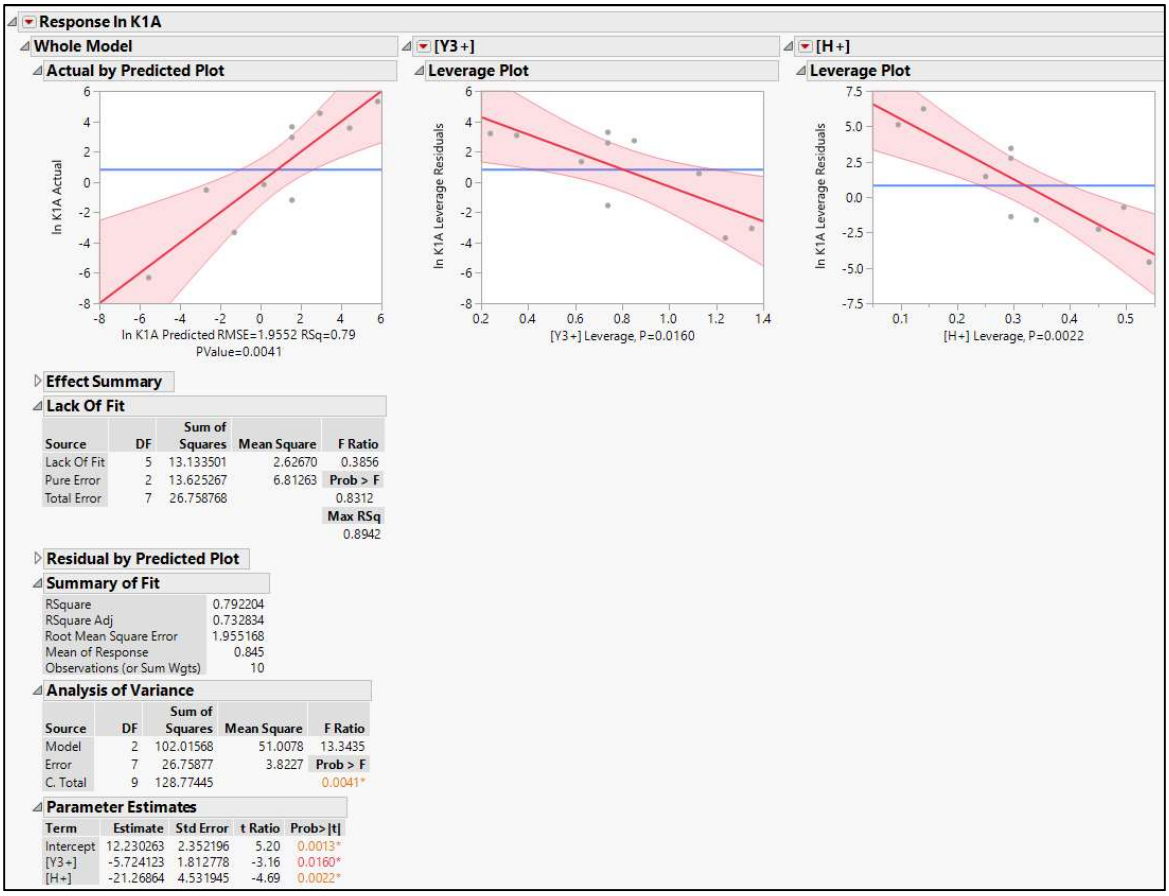

Source	DF	Sum of Squares	Mean Square	F Ratio
Lack Of Fit	5	13.133501	2.62670	0.3856
Pure Error	2	13.625267	6.81263	Prob > F
Total Error	7	26.758768		0.8312
				Max RSq
				0.8942

RSquare	0.792204
RSquare Adj	0.732834
Root Mean Square Error	1.955168
Mean of Response	0.845
Observations (or Sum Wgts)	10

Source	DF	Sum of Squares	Mean Square	F Ratio
Model	2	102.01568	51.0078	13.3435
Error	7	26.75877	3.8227	Prob > F
C. Total	9	128.77445		0.0041*

Term	Estimate	Std Error	t Ratio	Prob>|t|
Intercept	12.230263	2.352196	5.20	0.0013*
[Y3+]	-5.724123	1.812778	-3.16	0.0160*
[H+]	-21.26864	4.531945	-4.69	0.0022*

Figure 20: Linear Least Squares Regression for ln K_{1A}

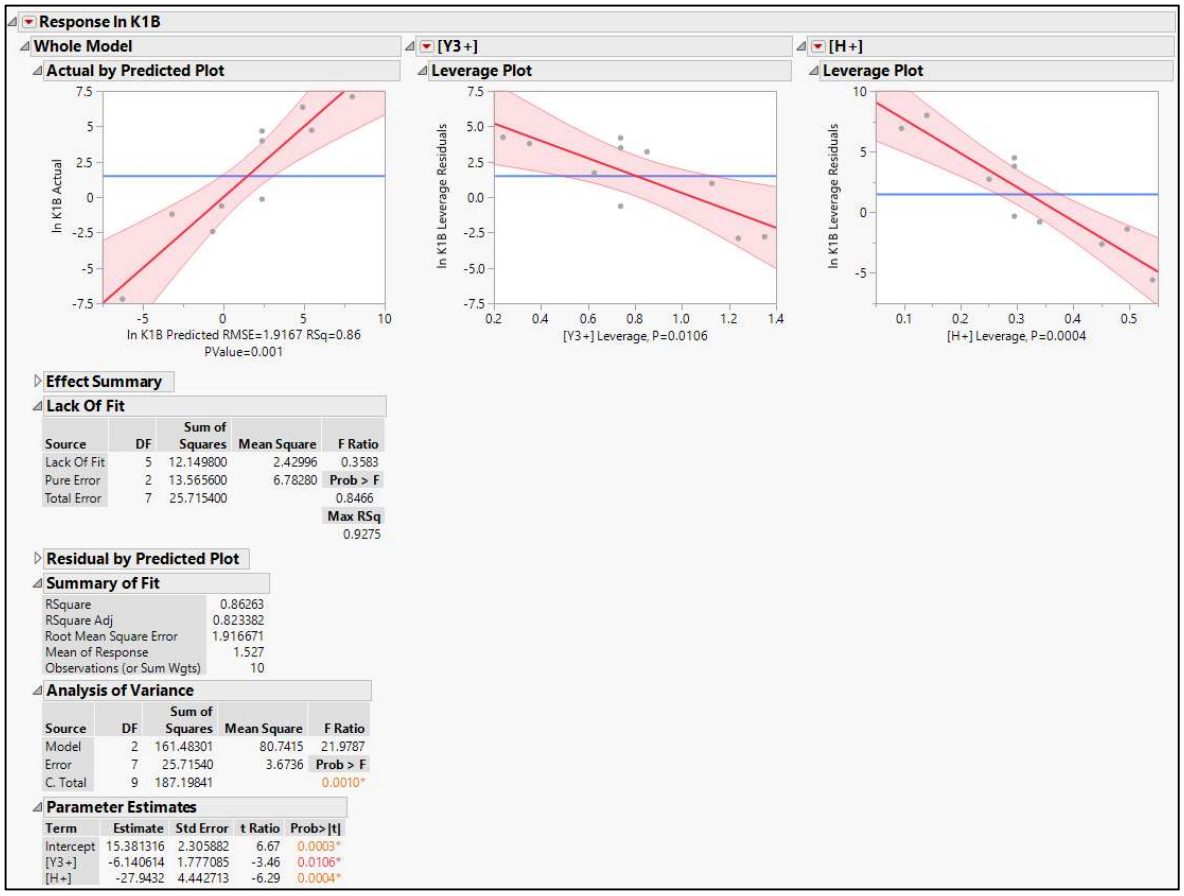

Figure 21: Linear Least Squares Regression for ln K_{1B}

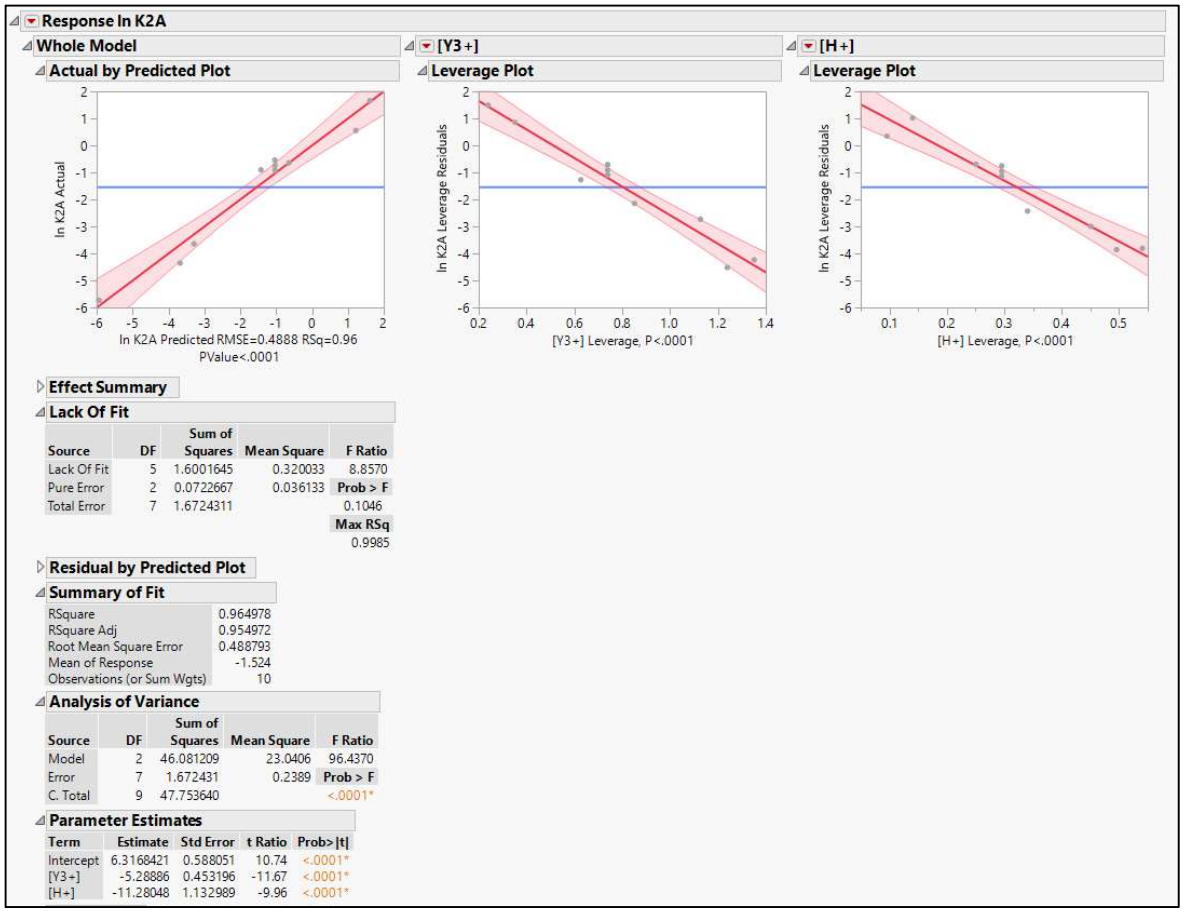

Figure 22: Linear Least Squares Regression for ln K_{2A}

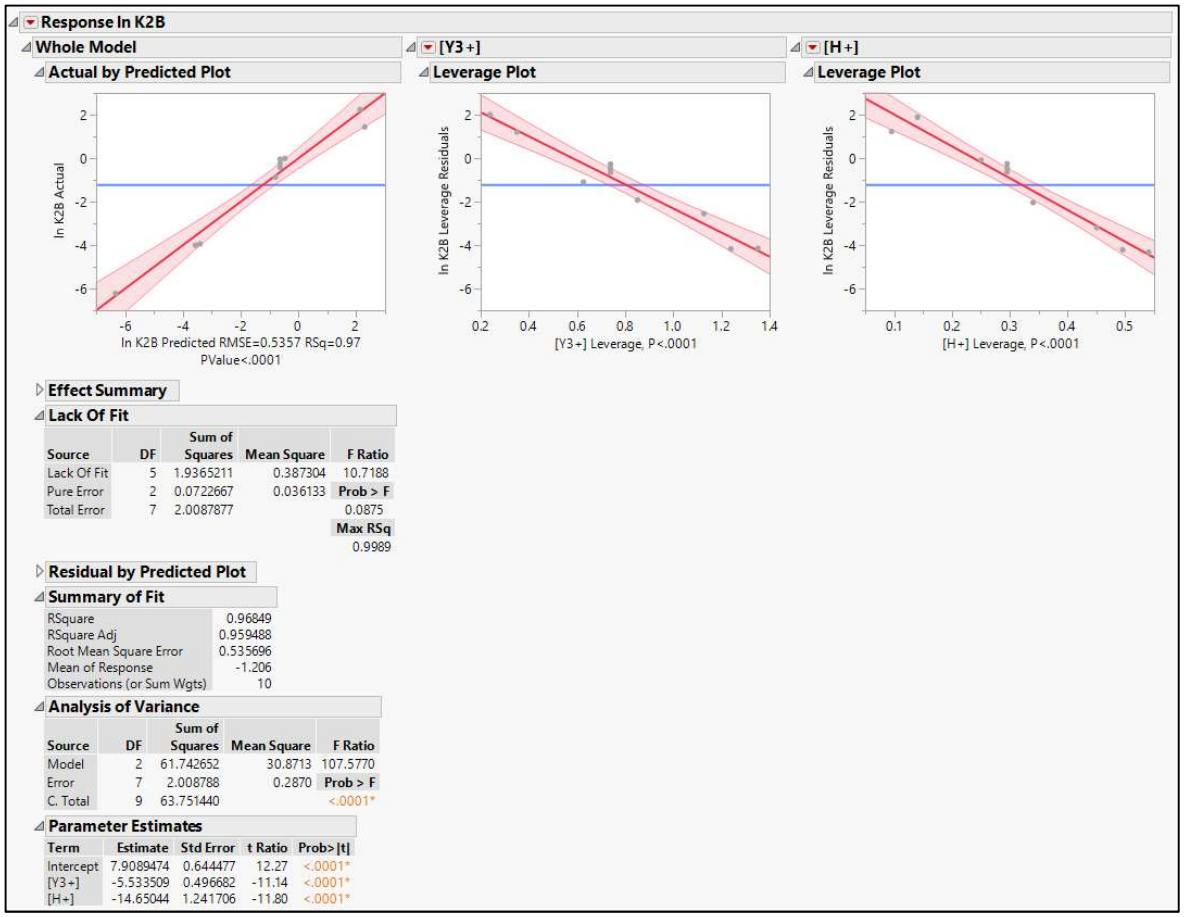

Figure 23: Linear Least Squares Regression for ln K_{2B}

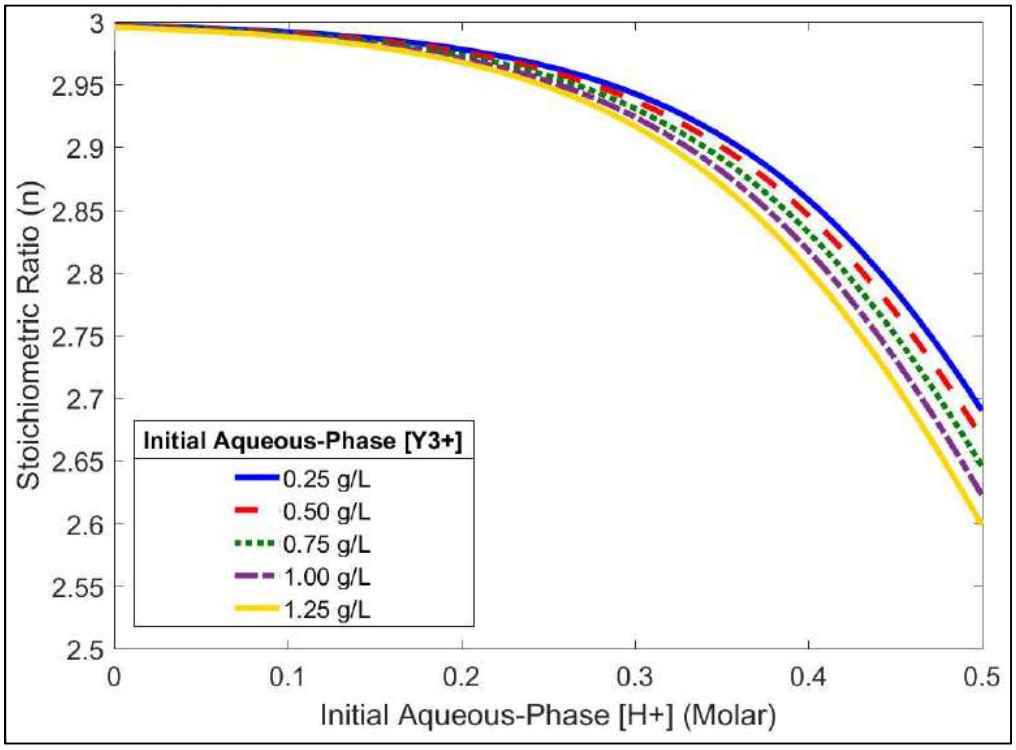

Figure 24: Stoichiometric Ratio vs. Aqueous-Phase Ion Concentration – Visualization of Equation (46)

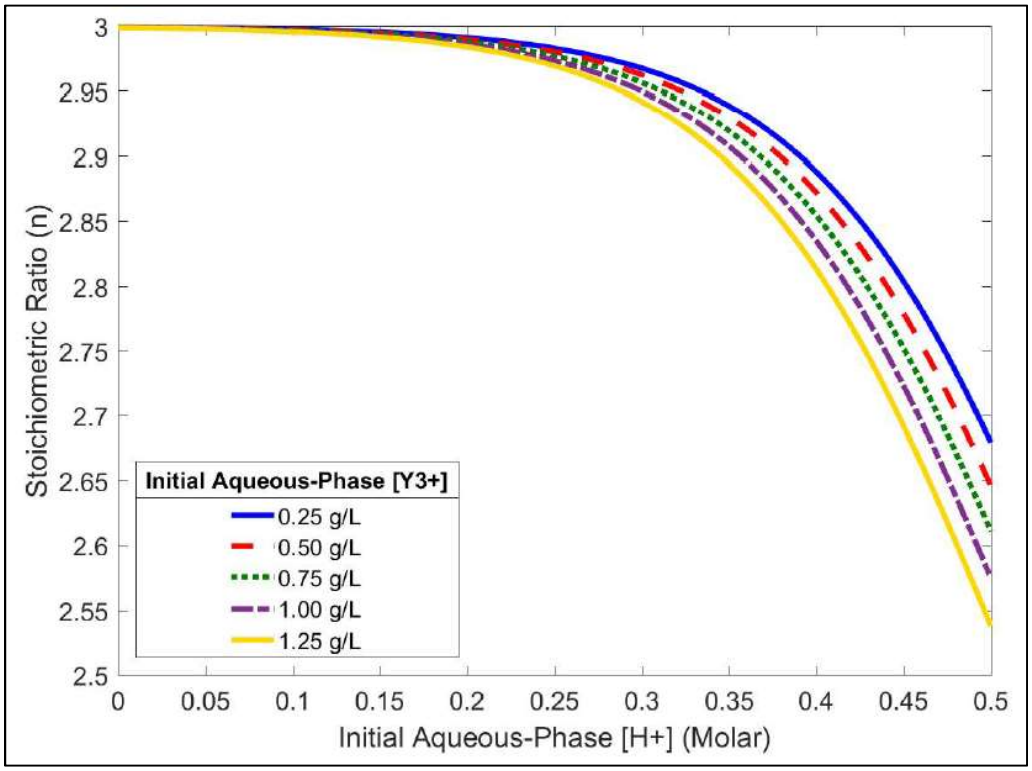

Figure 25: Stoichiometric Ratio vs. Aqueous-Phase Ion Concentration Using Activity Coefficients – Visualization of Equation (47)

CONCLUSION

Three process parameters – extraction rate coefficient, loading ratio, and stoichiometric ratio – were modeled for extracting yttrium from acidic solutions via DEHPA. A statistical model and a theoretical model were developed for the extraction rate coefficient. The first model predicts the extraction rate coefficient for a given extractant concentration and organic phase flow fraction whereas the second model yields the desired output if these two inputs plus the organic phase dynamic viscosity are known. Recycling the organic phase increased the extraction rate coefficient. Recycling could be a promising way to utilize extractants with high distribution coefficients to concentrate extracted metal ions. The extraction rate coefficient achieved a maximum value over the range of extractant concentrations used. Low extraction rate coefficients at high extractant concentrations were attributed to high viscosity due to high metal loading and low organic-phase diffusion. For systems where the resistance to mass transfer resides within the organic phase, it is recommended to operate the process at the greatest extractant concentration that does not yield viscosity effects.

All solvent extraction processes have an optimum extraction concentration corresponding to a maximum loading ratio. By operating at the optimum extractant concentration, the extractant is used most effectively. Using additional extractant beyond the optimum may decrease the economic viability of the extraction process – especially for costly extractants. Equations relating the loading ratio to the Murphree efficiency have been presented and the limitations of solely using the Murphree efficiency have been discussed. A procedure was introduced to calculate the optimum extractant concentration and to predict the loading ratio for any solvent extraction system. The validity of the procedure was confirmed by employing it to accurately predict the actual loading ratios for the extraction rate coefficient study. Sample calculations were provided to indicate the need to consider a high loading ratio as a targeted metric during process design. To achieve a higher loading ratio, it is recommended to operate nearer to the optimum extractant concentration rather than to increase the process efficiency.

The stoichiometric ratio for yttrium extraction from hydrochloric acid into DEHPA was modeled as a function of two simultaneous equilibrium equations. It was confirmed that the stoichiometric ratio was lower than the theoretical value of three and that chloride molecules entered the organic phase via complexation to reduce the stoichiometric ratio. A designed experiment was conducted to model the stoichiometric ratio in terms of the initial hydrogen ion and yttrium ion concentrations (conditions before equilibrium contact). The stoichiometric ratio was thus predicted for the range of experimental conditions. It was determined that the aqueous-phase activity coefficients add minimal precision to the estimates of the equilibrium coefficients and therefore add little to the estimates of the stoichiometric ratio. It is recommended to describe the system without employing activity coefficients to reduce the model parameters. Overall, it was determined that increasing the aqueous-phase hydrogen ion concentration (employing hydrochloric acid with a high molarity) yielded additional chloride molecules in the organic phase. Increasing the aqueous-phase yttrium ion concentration yielded a similar effect but to a lesser degree. The O:A yielded a negligible effect on the equilibrium constant and therefore no effect on the stoichiometric ratio.

These three parameters have been used as metrics to quantify extraction processes. These three independent studies addressed the scope of each parameter and which factors are most influential. Modeling each parameter has provided information regarding the factors affecting the processes and how these factors may be altered to achieve the desired extraction results.

VITA

David DeSimone earned a Bachelor of Arts in Anthropology and a Bachelor of Science in Civil/Environmental Engineering from the University of Rhode Island in 2006. After working as a design engineer in Baltimore, Maryland, he returned to academia to study Plastics Engineering at the University of Massachusetts – Lowell. Focusing on renewable resources and biomaterials, he earned a Master of Science in 2011. He was employed in the polymer processing industry for several years before returning to academia to pursue a Doctor of Philosophy in Chemical Engineering and a Master of Science in Statistics. While at the University of Tennessee, he focused his research on separation science. He intends to apply separation principles to industrial applications where pollution and other environmental concerns pose current challenges.

Having earned the rank of sergeant, David is a veteran of the United States Army National Guard. He enjoys international and domestic travel. As an avid cyclist, he has ridden his bicycle across the United States. He lives with his wife, Betsy, and their dog, Charlie.